Polycystine radiolarians in the Greenland–Iceland–Norwegian Seas: species and assemblage distribution

Giuseppe Cortese, Kjell R. Bjørklund & Jane K. Dolven

SARSIA

Cluster analysis and Q-mode factor analysis have been applied to polycystine radiolarian census data from 160 core-top samples. This allowed us to recognize four faunal assemblages in the Greenland–Iceland–Norwegian Seas, each related to different oceanographic conditions. A regression equation for deriving palaeotemperatures from these assemblages has also been developed. The standard error of estimate for this equation is ±1.2°C. The relative abundance of the species having the higher loadings in the core-top assemblages has been mapped, in order to identify and analyse water mass and environmental requirements for these species. Cluster analysis has also been performed on the same data set, providing results which are in good harmony with those derived by Q-mode factor analysis.

Giuseppe Cortese, Alfred Wegener Institute for Polar and Marine Research (AWI), Columbusstrasse, P.O. Box 120161, DE-27515 Bremerhaven, Germany.
Kjell R. Bjørklund & Jane K. Dolven, Paleontological Museum, University of Oslo, Sars gate 1, NO-0562 Oslo, Norway.
E-mail: gcortese@awi-bremerhaven.de; k.r.bjorklund@nhm.uio.no; j.k.l.dolven@nhm.uio.no

INTRODUCTION

The biogeographical distribution of microfossil species has been widely used in palaeontology in order to recognize faunal provinces and trace their position through time. When trying to extract palaeo-environmental information (e.g. the correlation between the relative percentage of a species and water temperature, or any other environmental variable) from a species' relative abundance at different stations, a simple x–y graph can be used as a rudimentary tool.

Increasingly more complex data sets containing a high number of species and stations require more sophisticated techniques, such as those that have been developed in the last decades to allow the description, simplification and interpretation of vast data sets. These so-called "multivariate techniques" (principal component analysis, correspondence analysis, cluster analysis, among others) are based on different algorithms, and can therefore be used jointly to stress different aspects of the data set, and to draw different, but closely related, conclusions.

In this paper we will use the factor analysis method (Imbrie & Kipp 1971) together with cluster analysis and describe what can be gained by the application of these methods to radiolarian census data from the surface sediments of the Greenland–Iceland–Norwegian (GIN) Seas.

Transfer functions for estimating mean surface ocean temperatures for the Norwegian Sea have been derived for planktonic foraminifera (Kellogg 1976), diatoms (Koç-Karpuz & Schrader 1990; Koç & al. 1993) and radiolarians (Bjørklund & al. 1998). The planktonic foraminifera assemblage (Kellogg 1976) of the GIN Seas is almost monospecific, with 95% *Neogloboquadrina pachyderma* (dextral) (Ehrenberg), while *Neogloboquadrina pachyderma* (sinistral) (Ehrenberg) and four additional species are common: *Globigerina bulloides* d'Orbigny, *Globigerina quinqueloba* Natland, *Globorotalia inflata* (d'Orbigny), and *Globigerinita glutinata* (Egger). Koç-Karpuz & Schrader (1990) used about 70 species to define surface diatom associations from the North Atlantic and the GIN Seas, and to extract palaeotemperature estimates for the last 13.5 ^{14}C ka (Koç & al. 1993, 1996).

Bjørklund & al. (1998) identified 75 radiolarian taxa in the GIN Seas surface sediments, while Samtleben & al. (1995) reported on 50 species from the sediment and 60 species from the plankton. In this study we have identified 114 radiolarian taxa, making the radiolarians the most diversified microplankton group, both in plankton and sediments, in the GIN Seas. The radiolarian data set developed by Bjørklund & al. (1998) was used to derive a palaeotemperature transfer function that was applied to a 13.5 ka long record from the southeastern Norwegian Basin (Dolven 1998).

In the present work we develop a new palaeotemperature equation for the GIN Seas, based on poly-

cystine radiolarians. This represents a considerable improvement over previously published work, as the current study is based on 114 taxa [compared with 75 taxa in Bjørklund & al. (1998)] and 160 core-top samples [compared with 63 samples in Bjørklund & al. (1998) and Dolven (1998)].

We include in the reference data set a greater geographical area (large portions of the Greenland Sea and the northern North Atlantic were not covered in previous studies) and a larger temperature range than in Bjørklund & al. (1998). By doing so, we expand the range of applicability of the present calibration data set, and improve the accuracy of palaeotemperature estimates in the GIN Seas.

Moreover, it has now been possible to recognize a Greenland Sea–Lofoten Basin faunal assemblage that seems to be related not only to sea surface temperature, but also to a variety of oceanographic variables, such as basin bathymetry, sea ice regime and processes, and opal dissolution at the bottom.

MATERIAL AND METHODS

Most of the core-top material used in this study was obtained from Christian-Albrechts University, Kiel, Germany (collected on RVs *Polarstern* and *Meteor*), the topmost 1–2 cm of the Trigger weight cores from the core libraries at the Lamont-Doherty Earth Observatory, Columbia University (RV *Vema* cruises 23, 27, 28, 29, and 30), and the Department of Oceanography, University of Washington (USS *Edisto* 1963 cruise). Two additional core-tops were made available to us from the Geological Institute, University of Bergen (RV *Håkon Mosby* cruise 31).

The reference data set includes 160 stations (filled circles in Fig. 1, asterisks in Table 1), extends from the Fram Strait to the Rockall Plateau area, documenting all the temperature and oceanographic regimes included, in the study area, between *ca* 55 and 80°N. The core-top samples used for the reference data set were chosen (from a total of 344 core-tops available) based on three criteria, in order of importance:

- samples with low abundance or barren of radiolarian skeletons were excluded;
- samples with very low communalities, indicative of poor preservation or reworked faunas, in preliminary factor analysis runs were excluded;
- samples significantly extending the geographical coverage of the reference data set were included.

The techniques used to separate the radiolarian skeletons from the sediment have been described previously by Goll & Bjørklund (1974). The sediment was disaggregated using hydrogen peroxide, and a constant volume of the screened residue (45 µm mesh size) mounted on a slide with Canada Balsam. We counted, in arbitrarily selected fields of view, between 261 and 502 specimens identified to the species level or to the lowest level possible. The resulting numbers included Spumellarida indet. (not identified) and Nassellarida indet. These two groups are negligible in some areas, constituting less than 5% of the total fauna, while in other areas they can be quite significant in numbers, often mainly juveniles (in areas with high values of radiolarians g^{-1}, low opal refraction index) and fragmented larcoids (in areas with low values of radiolarians g^{-1}, high opal refraction index).

In total, 114 species have been recognized by transmitted light microscopy. The species that were treated statistically had to occur with more than 2% of the total fauna in at least one station, as recommended by Imbrie & Kipp (1971).

In the GIN Seas we have recognized three morphotypes of the genus *Pseudodictyophimus: P. gracilipes gracilipes, P. g. bicornis*, and *P. g. multispina*. We have not been consistent during our work in identifying the three *Pseudodictyophimus* morphotypes, so we have chosen to list them as the *Pseudodictyophimus gracilipes* group. Several species common in the warm and transitional water regimes of the North Atlantic (*Euchitonia* spp., *Lamprocyclas maritalis, Spongocore*
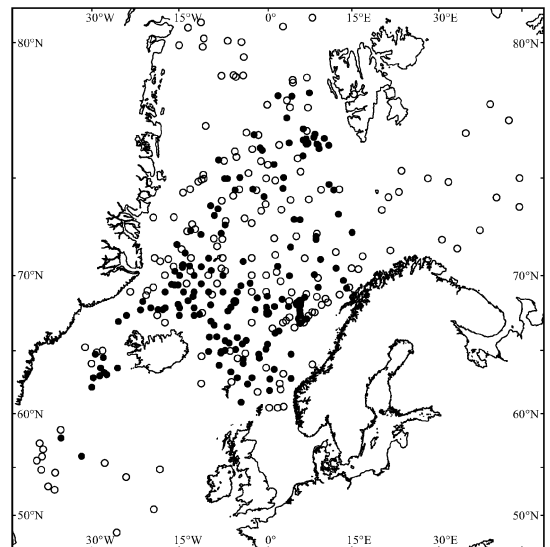
Fig. 1. Location of all the core-top samples examined in this study. The stations marked with a full circle have been included in the factor and cluster analyses.

Table 1. Geographical position of all the core-top samples examined in this study. Stations marked with an asterisk have been included in the Q-mode factor analysis run.

Latitude	Longitude	Station	Latitude	Longitude	Station	Latitude	Longitude	Station
65.768	−7.117	V23-58*	65.000	−7.818	V28-58*	77.183	−10.450	PS115
68.033	0.017	V23-59*	64.868	−7.868	V28-59*	80.067	−6.667	PS145
70.050	8.317	V23-60*	64.084	−4.033	V28-60*	80.133	−10.783	PS155
74.025	7.397	V23-61	64.418	−4.033	V28-60A*	80.600	−11.283	PS179
74.902	1.610	V23-62	64.907	−29.291	V29-206	80.450	−13.533	PS217
77.959	0.204	V23-63	69.261	−19.509	V29-207	79.883	−11.000	PS218
77.863	7.271	V23-64	63.969	−8.200	V29-208*	79.933	−15.033	PS234
78.336	15.200	V23-65	65.601	−6.484	V29-209*	67.702	7.960	PS16046
76.990	7.082	V23-66	66.735	−6.735	V29-210*	68.833	12.750	PS16319
75.605	0.284	V23-67	67.785	−6.668	V29-211*	72.023	−7.585	PS23362
72.867	−2.499	V23-68	70.150	−7.334	V29-212	70.815	−4.012	PS23364*
72.072	1.401	V23-69	74.351	−14.367	V29-213	70.535	1.992	PS23365*
70.987	6.691	V23-70	72.969	−6.985	V29-214	72.030	8.575	PS23367*
69.262	14.399	V23-71	75.927	−5.117	V29-215	72.323	8.802	PS23372
69.240	13.865	V23-72*	73.810	−0.095	V29-216	60.517	0.522	PS14904
68.548	2.718	V23-73*	68.384	−5.418	V29-218	60.517	2.032	PS14910
68.187	−9.601	V23-74*	68.384	−5.451	V29-219K*	60.625	3.008	P14918
64.802	−1.317	V23-75*	65.167	−0.067	V29-220*	63.273	2.992	PS14940
63.651	1.367	V23-76*	52.768	−36.585	V30-103	62.517	2.337	PS14943
62.651	−5.969	V23-77	53.100	−37.701	V30-104	61.983	0.545	PS14944*
62.518	−11.200	V23-78	54.518	−36.501	V30-105	55.475	−27.895	PS17050
63.449	−6.130	V27-40*	54.802	−38.885	V30-106	56.162	−31.990	PS17051*
62.493	−3.264	V27-41*	55.701	−39.668	V30-107	48.037	−25.837	PS17056
61.843	−1.464	V27-42	56.100	−38.735	V30-108	77.498	3.562	PS17726*
65.022	−6.220	V27-44	57.367	−39.200	V30-110	76.520	3.958	PS17728*
66.048	−8.593	V27-45*	56.802	−38.551	V30-122	71.613	4.213	PS17732*
67.588	−11.521	V27-46*	57.868	−35.501	V30-125*	69.468	−16.382	PS21843*
68.463	−13.543	V27-47*	58.568	−35.501	V30-126	69.442	−15.295	PS21846*
69.439	−15.900	V27-48*	64.067	−30.217	V30-128	70.253	−15.823	PS21852*
70.249	−13.067	V27-49	67.501	−15.067	V30-130*	70.600	−14.540	PS21855*
70.389	−7.757	V27-50	66.852	−9.033	V30-131*	70.640	−14.452	PS21856*
70.394	−7.787	V27-51	65.067	−7.134	V30-132*	70.480	−14.505	PS21857*
68.820	−9.327	V27-52	65.134	−5.301	V30-133*	72.300	−11.303	PS21873*
69.546	−2.820	V27-53*	64.468	−4.952	V30-134	72.547	−12.255	PS21875
73.109	−3.713	V27-54	70.301	−9.551	V30-135*	72.807	−12.773	PS21876
74.496	−4.658	V27-55	70.935	−16.935	V30-136	72.478	−13.067	PS21877*
76.159	−5.399	V27-56	71.484	−14.635	V30-137	73.252	−9.015	PS21878*
74.466	−1.691	V27-57	75.768	−7.267	V30-138	73.592	−8.397	PS21882*
73.541	2.665	V27-58	75.234	−3.050	V30-139	73.733	−9.625	PS21892*
73.070	4.822	V27-59*	76.418	2.251	V30-140	75.813	−8.258	PS21894*
72.184	8.581	V27-60*	77.868	4.134	V30-141	74.527	−2.335	PS21900*
71.321	12.068	V27-61	78.301	2.033	V30-142*	76.918	−3.383	PS21905
70.406	14.788	V27-62	76.284	9.117	V30-143*	76.842	−2.150	PS21906*
70.424	12.077	V27-63*	76.685	6.868	V30-144*	76.320	−1.072	PS21908*
73.516	20.000	V27-64	70.184	1.818	V30-145	75.617	1.317	PS21910*
74.381	22.977	V27-65	69.635	2.501	V30-146	75.050	2.967	PS21911*
71.999	30.409	V27-66	68.852	6.985	V30-147	74.567	2.900	PS21912*
72.498	37.000	V27-67	67.685	8.401	V30-148	74.483	−5.407	PS21913*
74.501	12.658	V27-68	68.568	10.284	V30-149	73.967	−7.663	PS21914
76.700	10.012	V27-69*	68.685	8.785	V30-150	68.420	4.008	PS23055
78.903	7.053	V27-70	71.084	16.701	V30-151	68.093	1.425	PS23065*
78.833	4.633	V27-71	74.835	31.551	V30-153	68.167	9.587	PS23240
78.738	4.636	V27-72	77.384	41.985	V30-154	67.657	5.815	PS23300*
76.499	7.047	V27-73	75.017	44.033	V30-155	71.292	−14.070	PS23346*
76.466	6.908	V27-74*	73.668	43.818	V30-156	65.530	−4.150	PS23359*
78.274	4.441	V27-75*	71.518	33.067	V30-158	72.778	−7.145	PS23361*
76.424	10.802	V27-76*	74.117	39.868	V30-159	67.010	2.917	PS23373
74.488	9.511	V27-77	77.985	38.752	V30-160	74.738	10.870	PS23385*
75.296	5.944	V27-78	76.902	34.551	V30-161	76.437	9.000	PS23398*

Table 1. Continued.

Latitude	Longitude	Station	Latitude	Longitude	Station	Latitude	Longitude	Station
78.119	3.625	V27-79	75.334	23.434	V30-162	72.352	−7.813	PS23400*
78.392	7.424	V27-80*	72.401	14.818	V30-163*	68.737	0.155	PS23402*
76.247	−2.394	V27-81	69.835	8.969	V30-164	71.413	21.490	PS23404
74.995	−10.808	V27-82	68.969	4.418	V30-165	75.000	28.003	PS23407
74.194	−5.716	V27-83	67.000	6.534	V30-166	65.798	−3.510	PS23411*
68.630	−1.596	V27-84*	67.000	5.852	V30-167*	54.835	−18.380	PS23413
67.362	4.027	V27-85	67.267	5.835	V30-168	50.673	−19.435	PS23417
66.608	1.119	V27-86	67.501	5.852	V30-169*	74.130	21.147	PS23428
62.937	4.281	V27-93*	67.267	7.017	V30-170*	76.475	8.737	PS23453*
66.289	1.493	V27-94*	67.468	7.367	V30-171	76.748	8.195	PS23454*
67.135	3.481	V27-95	68.401	5.852	V30-172	76.867	8.405	PS23455*
61.010	−4.339	V27-96*	68.334	5.752	V30-173	77.067	6.363	PS23456*
64.785	−29.568	V28-14*	68.167	5.752	V30-174	76.637	6.405	PS23457*
65.284	−31.334	V28-15	67.852	5.768	V30-175*	75.992	6.357	PS23458*
67.100	−25.618	V28-16*	67.167	6.084	V30-176	75.875	5.482	PS23459
67.500	−24.233	V28-17*	54.067	−24.184	V30-177	66.670	4.913	PS23467
68.785	−20.768	V28-18	67.501	−18.835	ED-1	71.633	−8.450	PS23478
68.217	−15.267	V28-19*	67.000	−17.501	ED-2	67.892	−17.920	PS23481*
70.802	−18.317	V28-20	69.000	0.000	ED-12	67.890	−18.763	PS23482*
71.768	−15.501	V28-21*	69.000	−2.501	ED-13	67.658	−11.077	PS23488
72.434	−13.651	V28-22	69.000	−5.000	ED-14*	67.505	−12.502	PS23489*
74.518	−13.117	V28-23	69.000	−7.501	ED-15*	65.032	−28.282	PS23516
75.167	−10.868	V28-24	69.501	−8.501	ED-16	64.542	−28.203	PS23518*
76.818	−1.334	V28-25	69.000	−10.000	ED-17*	64.798	−29.597	PS23519*
76.217	−0.701	V28-26*	69.501	−11.251	ED-18*	63.762	−28.658	PS23522*
75.752	−0.885	V28-27	70.000	−10.000	ED-19	62.250	−30.220	PS23523*
73.484	−0.835	V28-28	70.000	−7.501	ED-21*	63.003	−29.903	PS23524*
72.184	5.267	V28-29	70.000	−2.501	ED-24	63.248	−27.597	PS23525*
71.167	1.618	V28-30	70.000	0.000	ED-25	63.398	−28.062	PS23526*
66.451	2.167	V28-31*	71.000	−2.501	ED-27	63.163	−28.840	PS23528*
64.785	4.301	V28-32*	71.000	−7.501	ED-29	63.740	−25.740	PS23536*
62.902	0.585	V28-33*	71.000	−10.000	ED-30*	62.050	2.502	PS23537
64.835	−3.585	V28-34	71.000	−13.000	ED-32	75.000	−0.007	PS23548
67.117	−9.568	V28-35*	71.000	−19.251	ED-34	75.057	−4.598	PS23549*
68.718	−12.718	V28-36*	70.501	−16.000	ED-36	69.060	−20.510	PS23553
72.067	−9.067	V28-37	70.551	−13.251	ED-37*	69.990	3.987	PS31/002*
69.384	−4.401	V28-38*	70.501	−11.251	ED-38*	74.943	−11.175	PS31/024
67.885	−1.935	V28-39*	70.000	−12.501	ED-39*	78.933	−5.195	PS37/008
67.635	0.251	V28-40	70.000	−15.000	ED-40*	78.975	−3.973	PS37/012
67.685	0.234	V28-41*	70.000	−17.501	ED-41	78.990	−5.665	PS37/014
68.084	3.852	V28-42*	69.000	−23.501	ED-43	78.965	−7.688	PS37/016
67.200	6.167	V28-43	69.000	−17.501	ED-47*	80.022	−4.248	PS37/021
68.668	6.618	V28-44*	69.000	−14.301	ED-49*	79.570	−3.873	PS37/022
68.334	10.735	V28-45	69.501	−13.752	ED-50	75.002	−6.760	PS44/019*
69.701	13.334	V28-46*	69.000	−12.501	ED-51*	74.853	−11.745	PS44/020
70.367	16.000	V28-47	68.000	−12.501	ED-52*	74.177	−0.392	PS2613*
73.334	12.484	V28-48*	68.000	−15.000	ED-53*	73.155	−19.485	PS2641
74.484	11.668	V28-49*	68.000	−17.501	ED-54*	75.005	−7.203	PS2616*
74.000	4.234	V28-50	68.000	−20.000	ED-55*	73.160	−15.967	PS2628
73.050	5.818	V28-51*	66.033	−9.868	ED-60*	67.868	−21.758	PS2644*
70.935	9.384	V28-52*	66.000	−5.000	ED-62*	68.395	−21.395	PS2645*
69.284	8.985	V28-53*	67.000	−2.501	ED-63	80.733	8.050	PS55/100
68.251	5.367	V28-54	64.000	8.000	ED-69	80.483	2.933	PS55/151
65.518	0.200	V28-55*	65.000	−10.000	ED-77*	64.500	−1.250	HM31-35*
68.033	−6.117	V28-56*	63.000	−2.501	ED-87*	63.750	0.000	HM31-37
64.635	−11.150	V28-57	63.000	−5.000	ED-88*			

puella, Theocorythium trachelium) are found in the GIN Seas. They are too rare to be of any importance as individual species, but as a warm water group they may show a more significant distribution pattern. We therefore grouped them as "Drift fauna" in our species list. Finally, *Spongotrochus glacialis, Spongopyle osculosa* and *Spongopyle resurgens* are common in our material. However, as most of them are juvenile stages, we have

not with confidence been able to separate these species. *Spongotrochus glacialis* being the most common species, we grouped these three spongodiscids as the *Spongotrochus* group.

Moreover, *Artostrobus annulatus* and *Cycladophora davisiana* have not been considered when developing the palaeotemperature regression equation, as it has been demonstrated that they live in intermediate or deep

Table 2. List of polycystine radiolarian species discussed in this study, with reference to Plates 1–4 for species with scaled varimax factor scores >1.

Radiolarian taxa referenced in this study	Plate 1	Plate 2	Plate 3	Plate 4
Actinomma leptoderma (Jørgensen) *longispina* Cortese and Bjørklund (1998)		5–7		
Actinomma leptoderma Jørgensen (1900)	21	1	10	
Actinomma boreale Cleve (1899)	22–24	2–4	6, 7, 11	
Actinomma medianum Nigrini (1967)				
Actinomma sp. 1				
Actinomma sp. 2			8, 9, 12	
Amphimelissa setosa Cleve (1899)	1–9	14–17		16, 17
Artobotrys borealis Cleve (1899)				8–11
Artostrobus annulatus Bailey (1856)				
Artostrobus joergenseni Petrushevskaya (1967)				
Ceratocyrtis galeus Cleve (1899)				
Ceratocyrtis histricosus Jørgensen (1905)				
Corocalyptra craspedota Jørgensen (1900)				27, 28
Cycladophora davisiana Ehrenberg (1862)				
Euchitonia spp.				
Eucyrtidium calvertense Martin (1904)				
Lamprocyclas maritalis Haeckel (1887)				
Larcoidea sp. 1			13–15	
Larcospira minor Jørgensen (1900)		8–11	1, 2	
Lipmanella xiphephorum Jørgensen (1900)				
Lithelius spiralis Haeckel (1862)				
Lithocampe platycephala Ehrenberg (1873)	15–20			
Lithomelissa hystrix Jørgensen (1900)				20–22
Lithomelissa setosa Jørgensen (1900)				1–7
Lithomelissa sp. aff. *L. stigi* Bjørklund (1976)				
Lithomelissa thoracites Haeckel (1862)				
Lithomitra lineata Ehrenberg (1839)				23–26
Phorticium pylonium (clevei) Haeckel (1887)		12, 13	5	18, 19
Phorticium sp. 1				
Plagiacantha arachnoides (Claparède, 1855)				
Plectacantha oikiskos Jørgensen (1905)				
Pseudodictyophimus gracilipes (Bailey) *bicornis* Ehrenberg (1873)	12, 13			12
Pseudodictyophimus gracilipes (Bailey) *multispinus* Bernstein (1934)	14			14, 15
Pseudodictyophimus gracilipes gracilipes Bailey (1856)	10, 11			13
Sethoconus (Artostrobus) tabulatus Ehrenberg (1873)				
Spongocore puella Haeckel (1887)				
Spongodiscus osculosus Dreyer (1889)			4	
Spongodiscus resurgens Ehrenberg (1854)				
Spongotrochus glacialis Popofsky (1908)			3	
Streblacantha circumtexta Jørgensen (1900)				
Streblacantha sp. 1				
Stylatractus sp. 1				
Theocorythium trachelium Ehrenberg (1873)				
Tholospyris gephyristes Hülsemann (1963)				

water masses. Six plankton stations (Cleve's slide collection at the Swedish Museum of Natural History, Stockholm), sampled during July–September 1898 in the study area (Bjørklund, unpublished data) confirm the subsurface habitat of *Artostrobus annulatus* and *Cycladophora davisiana*, as both species were absent from plankton tows shallower than 500 m water depth, while both were present in deeper tows.

After these selection criteria were applied, 34 species remained for further analyses. The 34 taxa included in the factor run in this study are shown in Tables 2 and 3, while the most important species in the four GIN Sea factor groups are shown in Plates 1–4. [The plates figure only taxa having high factor loadings in the present paper. Images and taxonomic references for rarer taxa from the study area are found in Bjørklund (1976), Schröder-Ritzrau (1995) and Bjørklund & al. (1998).]

The log-transform of the relative abundance of these species, $X_{log-transf} = \ln (X_\% + 1)$, was used as the input matrix for the Q-mode factor analysis.

Dietrich's (1969) summer water temperature data set was used as the source of surface hydrography information, as this atlas provides an accurate and realistic picture of the distribution of this variable in the GIN Seas. An evaluation of this data set, and why it was preferred over others, is presented in Bjørklund & al. (1998). Summer temperatures were used, as this is the most likely time of the year for radiolarians to reproduce, and the highest flux of radiolarian skeletons to the sediments will occur during the summer months.

In fact, in the GIN Seas, the highest opal, carbonate and particulate organic carbon fluxes are observed in the summer (Peinert & al. 2001). This high export season corresponds to late May until September in the

Table 3. Scaled varimax factor scores for the taxa used in this study. Absolute values higher than 1.000 are in bold.

	Factor 1	Factor 2	Factor 3	Factor 4
Actinomma leptoderma/boreale group	**1.615**	**4.588**	**−1.661**	0.721
Actinomma leptoderma longispina	−0.240	**1.861**	−0.823	−0.284
Actinomma medianum	0.019	−0.038	0.234	−0.074
Actinomma sp. 1	−0.022	−0.017	−0.050	0.177
Actinomma sp. 2	0.083	−0.188	**1.091**	−0.327
Amphimelissa setosa	**4.732**	**−1.252**	0.967	**−1.310**
Artobotrys borealis	0.072	−0.521	−0.221	**2.388**
Artostrobus joergenseni	0.897	−0.419	0.144	0.507
Ceratocyrtis galeus	0.026	0.026	−0.058	0.244
Ceratocyrtis histricosus	0.001	−0.053	−0.078	0.366
Corocalyptra craspedota	−0.196	−0.162	0.020	**1.036**
Drift fauna	−0.043	−0.037	0.225	0.132
Eucyrtidium calvertense	0.008	−0.058	0.271	−0.025
Larcospira minor	−0.409	**1.798**	**3.421**	0.015
Larcoidea sp. 1	−0.189	−0.270	**1.086**	0.990
Lipmanella xiphephorum	−0.054	−0.041	−0.058	0.380
Lithelius spiralis	−0.064	−0.105	0.032	0.408
Lithocampe platycephala	**1.731**	0.563	−0.273	0.865
Lithomelissa hystrix	−0.144	−0.237	0.020	**1.124**
Lithomelissa setosa	−0.040	−0.929	0.045	**3.683**
Lithomelissa sp. aff. *L. stigi*	−0.046	−0.023	−0.073	0.227
Lithomelissa thoracites	−0.056	−0.057	−0.056	0.374
Lithomitra lineata	0.145	−0.377	0.020	**1.217**
Phorticium pylonium (clevei)	−0.284	**1.477**	**1.956**	**1.273**
Phorticium sp. 1	0.015	−0.034	0.160	−0.046
Plagiacantha arachnoides	0.033	−0.053	−0.013	0.123
Plectacantha oikiskos	0.135	−0.110	−0.029	0.331
Pseudodictyophimus gracilipes group	**2.034**	−0.207	0.376	**1.577**
Sethoconus (Artostrobus) tabulatus	0.025	−0.014	−0.001	0.034
Spongotrochus glacialis group	−0.068	0.624	**3.294**	−0.296
Streblacantha circumtexta	−0.128	0.149	0.394	0.150
Streblacantha sp. 1	−0.110	−0.184	0.076	0.777
Stylatractus sp. 1	0.014	−0.089	0.398	−0.038
Tholospyris gephyristes	0.747	−0.078	−0.199	0.900

Summer sea surface temperature (SSST) = −7.64 * F1 − 8.68 * F2 + 0.04 * F3 + 5.52 * F4 + 13.66
Multiple correlation coefficient = 0.88
Standard error of estimate = ±1.2°C
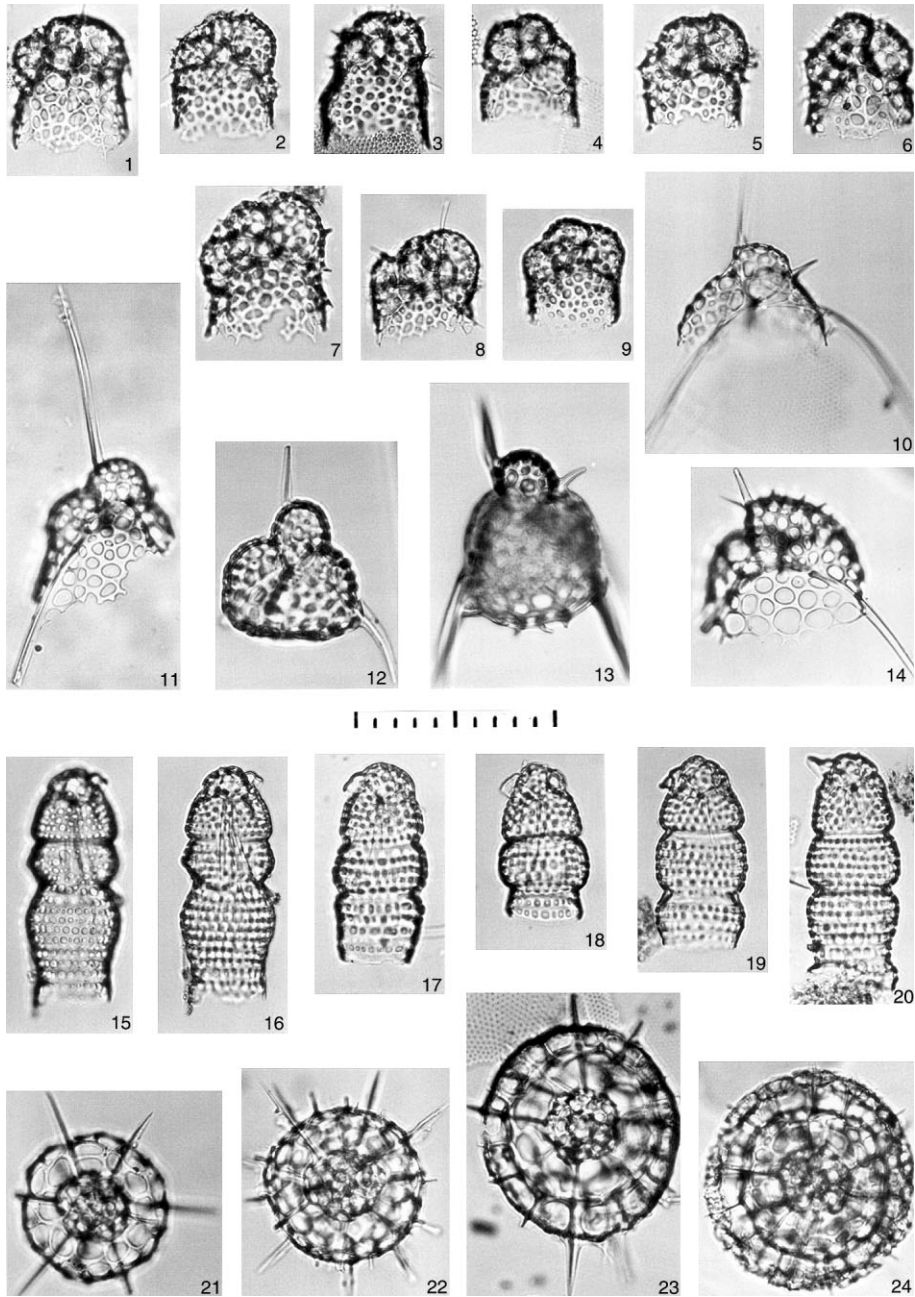
Plate 1. Factor 1 species with factor loading values (FLV) > 1. Scale: all 100 µm. (1)–(9) *Amphimelissa setosa* (Cleve) (FLV = 4.732). (1), (7)–(9) from V27-46; (2), (3) from V27-94; (4) from V29-220; (5), (6) from V27-49. (10)–(14) *Pseudodictyophimus gracilipes* (Ehrenberg) group (FLV = 2.034). (10), (11) *Pseudodictyophimus gracilipes gracilipes* (Bailey) from V27-94 and V27-60, respectively; (12), (13) *Pseudodictyophimus gracilipes bicornis* (Ehrenberg) from V27-60 and V27-94, respectively; (14) *Pseudodictyophimus gracilipes multispinus* (Bernstein) from V27-94. (15)–(20) *Lithocampe platycephala* (Ehrenberg) (FLV = 1.731). (15)–(19) from V27-60; (20) from V27-46. (21)–(24) *Actinomma leptoderma/boreale* group (FLV = 1.615). (21) *Actinomma leptoderma* (Jørgensen) from V29-220; (22)–(24) *Actinomma boreale* (Cleve) from V27-60, V29-220, V28-55, respectively.
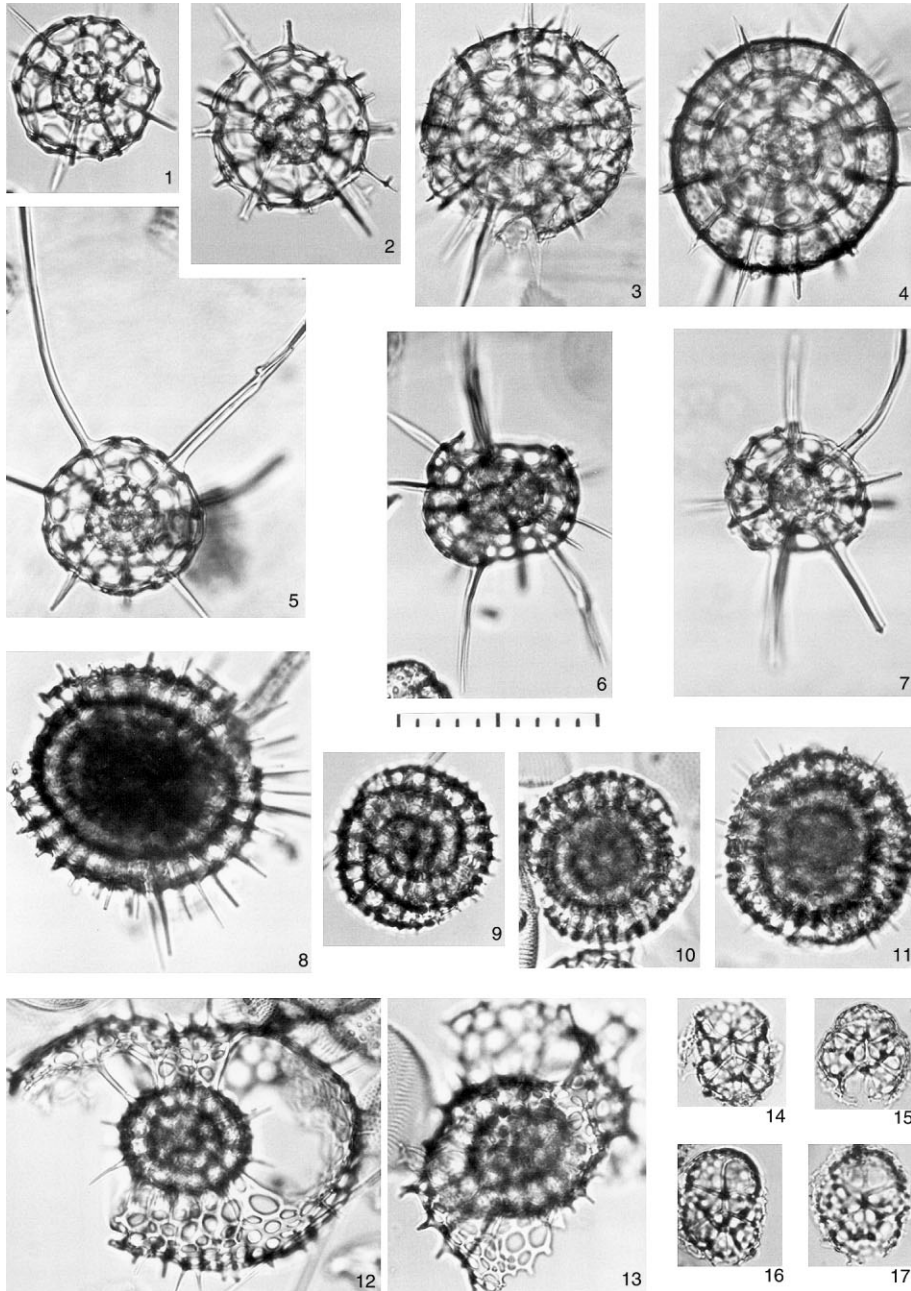
Plate 2. Factor 2 species with factor loading values (FLV) > 1. Scale: all 100 µm. (1)–(4) *Actinomma leptoderma/boreale* group (FLV = 4.588). (1) *Actinomma leptoderma* (Jørgensen) from V30-173; (2)–(4) *Actinomma boreale* (Cleve), (2) from V27-41, (3), (4) from V28-55. (5)–(7) *Actinomma leptoderma* (Jørgensen) *longispina* Cortese and Bjørklund (FLV = 1.861). (5), (6) from V27-94; (7) from V27-60. (8)–(11) *Larcospira minor* (Jørgensen) (FLV = 1.798). (8), (9) from V27-94. (10), (11) from V30-173. (12), (13) *Phorticium pylonium* (*clevei*) Haeckel (FLV = 1.477). (12) from V29-220; (13) from V27-94. (14)–(17) *Amphimelissa setosa* (Cleve) (FLV = −1.252); all from V27-46.
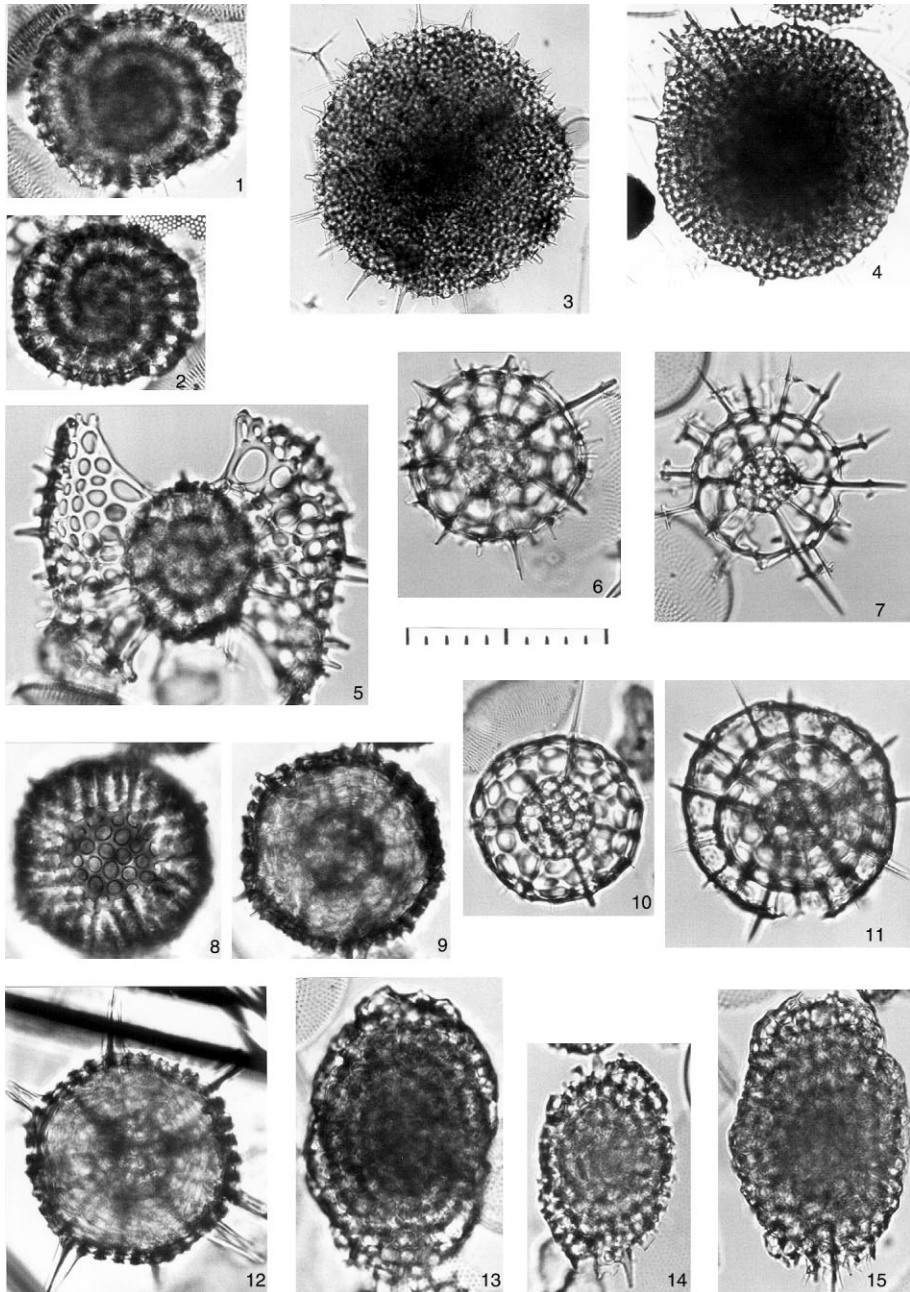
Plate 3. Factor 3 species with factor loading values (FLV) > 1. Scale: all 100 μm, except (3). (1), (2) *Larcospira minor* (Jørgensen) (FLV = 3.421); both from V29-220. (3), (4) *Spongotrochus glacialis* group (FLV = 3.294). (3) *Spongotrochus glacialis* from V28-55 (scale = 50 μm); (4) *Spongodiscus osculosus* from V28-55. (5) *Phorticium pylonium clevei* Haeckel (FLV = 1.956); from V30-173. (6), (7), (10), (11) *Actinomma leptoderma/boreale* group (FLV = −1.661); (10) *Actinomma leptoderma* (Jørgensen) from V30-173; (6), (7), (11) *Actinomma boreale* (Cleve), (7), (10) from V30-173, (11) from V27-60. (8), (9), (12) *Actinomma* sp. 2 (FLV = 1.091); all from K23413. (13)–(15) Larcoidea sp. 1 (FLV = 1.086); (13) from V29-220; (14), (15) from V30-173.
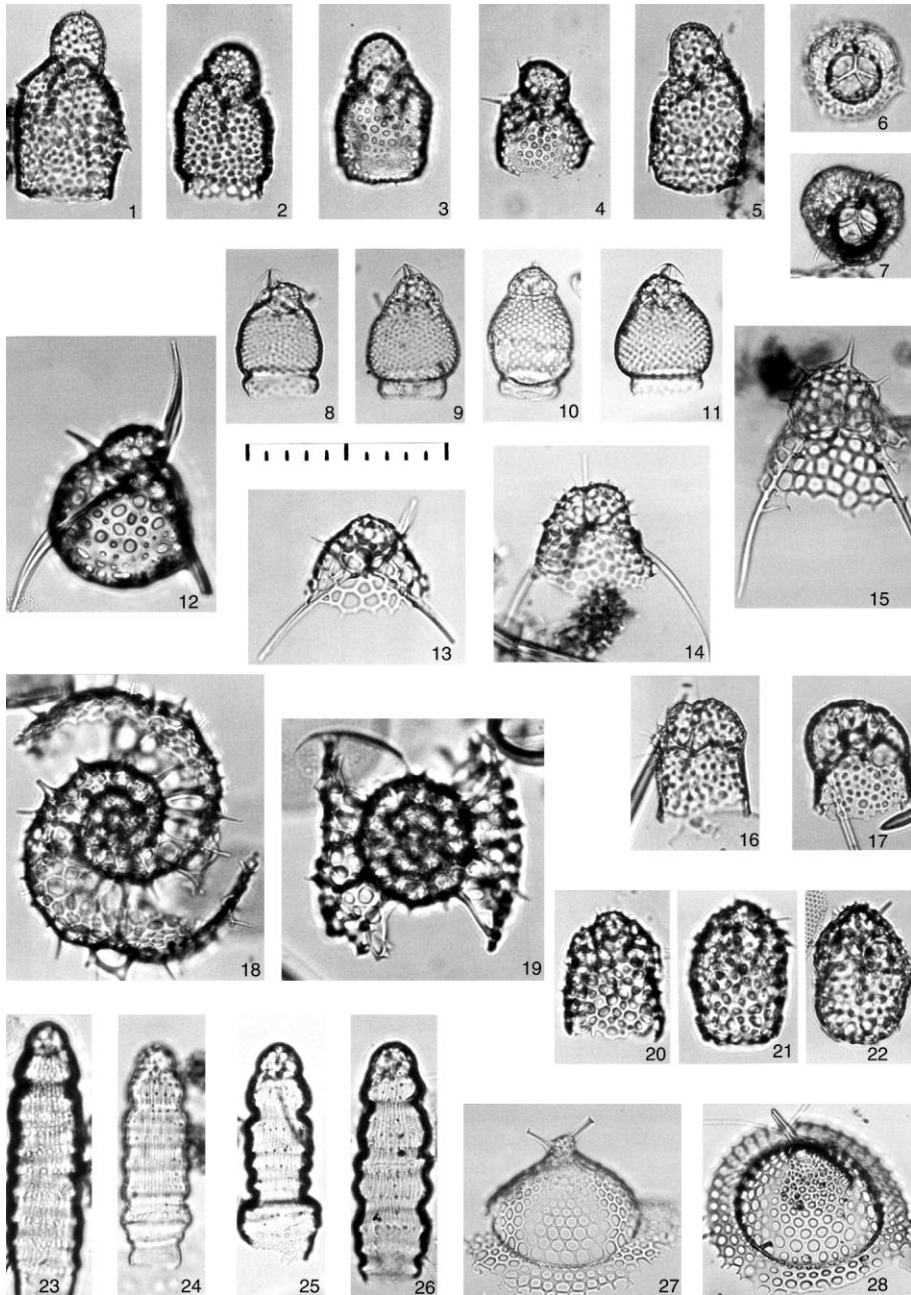
Plate 4. Factor 4 species with factor loading values (FLV) > 1. Scale: all 100 μm. (1)–(7) *Lithomelissa setosa* Jørgensen (FLV = 3.683); (1), (2), (4), (7) from V27-94; (3) from V29-220; (5) from V30-173; (6) from V28-55. (8)–(11) *Artobotrys borealis* (Cleve) (FLV = 2.388); (8), (9) from V29-220; (10), (11) from V23-94. (12)–(15) *Pseudodictyophimus gracilipes* group (FLV = 1.577). (12) *Pseudodictyophimus gracilipes bicornis* (Ehrenberg) from V27-94; (13) *Pseudodictyophimus gracilipes gracilipes* (Bailey) from V27-94; (14), (15) *Pseudodictyophimus gracilipes multispinus* (Bernstein) from V27-60. (16), (17) *Amphimelissa setosa* (Cleve) (FLV = −1.310). (16) from V30-173; (17) from V27-60. (18), (19) *Phorticium pylonium* (*clevei*) Haeckel (FLV = 1.273); both from V30-173. (20)–(22) *Lithomelissa hystrix* Jørgensen (FLV = 1.124). (20) from V27-60; (21), (22) from V27-94. (23)–(26) *Lithomitra lineata* (Ehrenberg) (FLV = 1.217). (23), (24) from V27-60; (25) from V27-94; (26) from V29-220. (27), (28) *Corocalyptra craspedota* Jørgensen (FLV = 1.036). (27) from V27-94; (28) from V29-219.
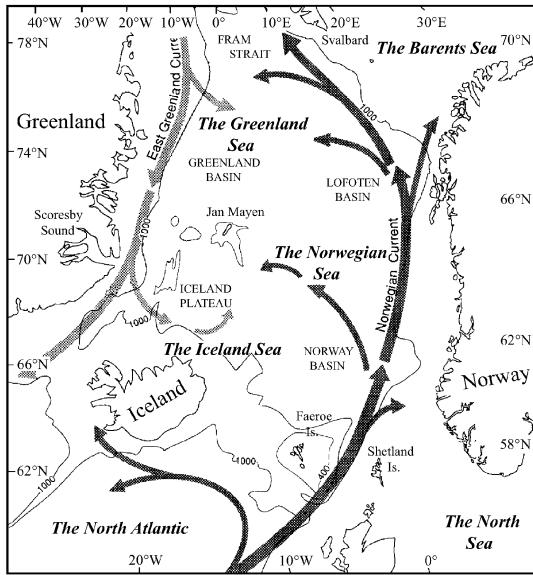
Fig. 2. Major surface currents in the Greenland, Iceland and Norwegian Seas. The dark arrows represent the warm Norwegian Current and the lighter arrows the cold East Greenland Current. Modified from Sejrup & al. (1995).

Greenland Sea, and from August until October in the Norwegian Sea. Therefore, microfossils in the surface sediments from the GIN Seas generally reflect the summer/autumn production maximum in the surface water masses (Matthiessen & al. 2001).

The main surface currents and the bottom topography of the study area are shown in Fig. 2.

Q-mode factor analysis (Imbrie & Kipp 1971) was used for the statistical treatment of the data set, using the software packages PalaeoToolBox and Mac Transfer (Sieger & al. 1999).

Q-mode factor analysis can be described as a rotation of data points in multidimensional space, in order for the longest axis (the one with the greatest variance) to be the first factor axis, the second longest axis, perpendicular to the first, is the second factor axis, and so on. An eigenvector (a series of component loadings for each taxon, indicating the relative importance of each taxon in the extracted principal component) is associated with each of these component axes. The faunal assemblages and species relative abundance maps have been produced by PanMap (Diepenbroek & al. 2000) and Arc View. The core-top data set has also been examined by means of cluster analysis, using the software package Past (Hammer & al. 2001), with an unweighted pair grouping method and a Spearman rank-order correlation coefficient.

Many similarity indexes can be used as input for cluster analysis. The evaluation of the characteristics of the input data set can help in choosing an appropriate similarity index. When dealing with fossil data, whose distribution can be affected by processes such as lateral transport, differential dissolution, winnowing, reworking, non-metric, quantitative similarity measures (e.g. Spearman rank-order correlation coefficient) should be used (Sneath & Sokal 1973). One of the advantages of a
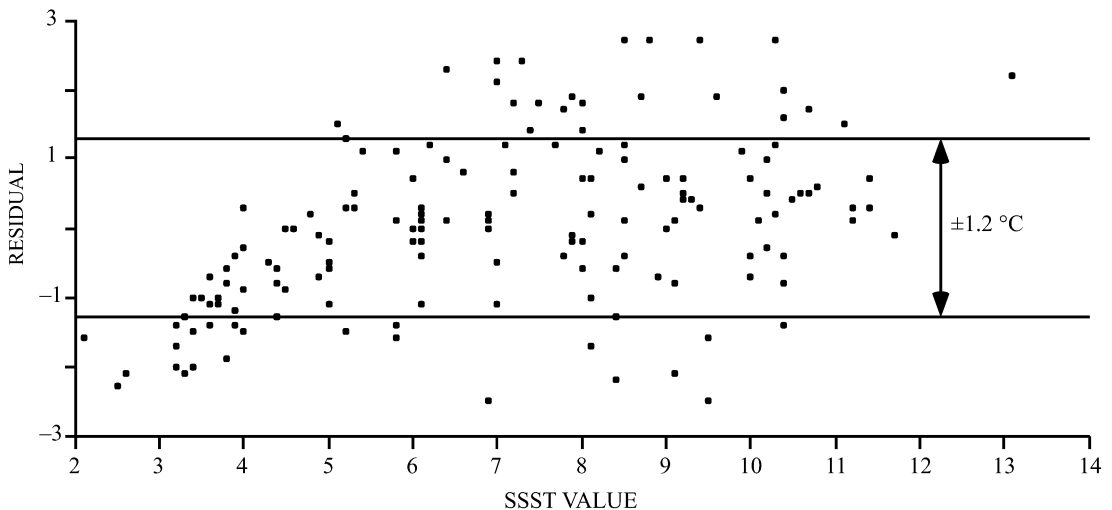
Fig. 3. Measured summer sea surface temperatures (SSST) versus residuals (estimated minus measured SSST) for all core-top stations. The standard error of estimate ($\pm1.2°C$) is also shown.

Table 4. Station varimax factor components matrix for the four polycystine radiolarian factors/assemblages used in this study. The communality for each station as well as the variance and cumulative variance for each factor are also reported.

Station	Communality	Factor 1	Factor 2	Factor 3	Factor 4	Station	Communality	Factor 1	Factor 2	Factor 3	Factor 4
ED-14	0.950	0.629	0.321	0.145	0.656	K44/19	0.978	0.364	0.879	0.140	0.232
ED-15	0.963	0.721	0.458	0.238	0.419	K14944	0.907	0.054	0.551	0.748	0.203
ED-17	0.976	0.949	0.216	0.047	0.161	K17051	0.844	0.053	0.369	0.825	0.156
ED-18	0.988	0.972	0.173	0.005	0.120	K17726	0.971	0.385	0.846	0.128	0.299
ED-21	0.984	0.874	0.415	0.011	0.220	K17728	0.952	0.378	0.854	0.060	0.275
ED-30	0.972	0.952	0.196	0.065	0.154	K17732	0.923	0.203	0.855	0.279	0.270
ED-37	0.979	0.911	0.338	−0.048	0.183	K21843	0.963	0.941	0.222	0.056	0.157
ED-38	0.985	0.929	0.258	0.036	0.235	K21846	0.966	0.222	0.910	0.229	0.189
ED-39	0.984	0.963	0.215	−0.007	0.100	K21852	0.970	0.307	0.908	0.078	0.210
ED-40	0.977	0.929	0.310	−0.031	0.129	K21855	0.960	0.857	0.374	0.029	0.293
ED-47	0.987	0.944	0.287	−0.038	0.113	K21856	0.938	0.794	0.512	−0.030	0.211
ED-49	0.983	0.925	0.319	−0.059	0.148	K21857	0.948	0.474	0.832	0.064	0.167
ED-51	0.979	0.970	0.148	0.025	0.126	K21873	0.957	0.268	0.880	0.276	0.184
ED-52	0.987	0.971	0.179	0.000	0.115	K21877	0.973	0.318	0.891	0.187	0.206
ED-53	0.974	0.914	0.325	−0.015	0.178	K21878	0.964	0.227	0.905	0.256	0.167
ED-54	0.984	0.950	0.209	0.057	0.186	K21882	0.975	0.270	0.915	0.170	0.188
ED-55	0.965	0.882	0.393	0.050	0.175	K21892	0.975	0.241	0.911	0.235	0.178
ED-60	0.963	0.927	0.161	0.040	0.275	K21894	0.929	0.185	0.896	0.256	0.162
ED-62	0.949	0.663	0.468	0.220	0.491	K21900	0.942	0.352	0.878	0.087	0.199
ED-77	0.903	0.822	0.218	0.207	0.371	K21906	0.961	0.229	0.891	0.291	0.177
ED-87	0.900	0.810	0.128	0.066	0.472	K21908	0.904	0.839	0.343	0.114	0.263
ED-88	0.971	0.844	0.176	0.192	0.438	K21910	0.977	0.426	0.855	0.066	0.244
V23-58	0.946	0.901	0.146	0.116	0.318	K21911	0.919	0.883	0.291	0.037	0.229
V23-59	0.961	0.651	0.355	0.261	0.587	K21912	0.935	0.426	0.838	0.036	0.226
V23-60	0.937	0.508	0.499	0.261	0.602	K21913	0.985	0.322	0.901	0.131	0.228
V23-72	0.941	0.275	0.549	0.342	0.669	K23065	0.978	0.160	0.803	0.513	0.212
V23-73	0.964	0.412	0.598	0.385	0.537	K23300	0.957	0.174	0.772	0.451	0.357
V23-74	0.981	0.923	0.313	0.033	0.175	K23346	0.955	0.340	0.881	0.182	0.173
V23-75	0.962	0.676	0.239	0.213	0.634	K23359	0.965	0.160	0.896	0.309	0.203
V23-76	0.930	0.565	0.340	0.253	0.656	K23361	0.967	0.274	0.879	0.243	0.245
V27-40	0.910	0.800	0.207	0.182	0.440	K23364	0.968	0.155	0.862	0.404	0.198
V27-41	0.850	0.502	0.268	0.453	0.566	K23365	0.985	0.214	0.866	0.345	0.265
V27-45	0.962	0.924	0.189	−0.004	0.268	K23367	0.980	0.213	0.930	0.209	0.164
V27-46	0.987	0.985	0.086	0.062	0.077	K23385	0.940	0.205	0.872	0.259	0.265
V27-47	0.949	0.943	0.243	−0.013	−0.010	K23398	0.977	0.196	0.878	0.338	0.229
V27-48	0.947	0.782	0.521	−0.148	0.206	K23400	0.969	0.352	0.858	0.158	0.288
V27-53	0.945	0.596	0.407	0.215	0.615	K23402	0.965	0.133	0.820	0.472	0.230
V27-59	0.965	0.830	0.361	0.020	0.380	K23411	0.957	0.206	0.873	0.268	0.286
V27-84	0.945	0.658	0.348	0.064	0.622	K23453	0.937	0.101	0.853	0.408	0.180
V27-93	0.876	0.397	0.346	0.165	0.756	K23454	0.965	0.222	0.882	0.264	0.262
V27-94	0.944	0.598	0.402	0.190	0.623	K23455	0.950	0.158	0.884	0.308	0.220
V28-14	0.888	0.474	0.159	0.528	0.599	K23456	0.959	0.262	0.859	0.241	0.307
V28-16	0.974	0.815	0.477	0.100	0.269	K23457	0.970	0.259	0.849	0.287	0.315
V28-19	0.963	0.948	0.223	−0.017	0.125	K23458	0.979	0.267	0.890	0.226	0.254
V28-31	0.909	0.527	0.363	0.194	0.680	K23481	0.975	0.643	0.698	0.171	0.215
V28-32	0.942	0.373	0.466	0.293	0.707	K23482	0.972	0.557	0.786	0.109	0.179
V28-33	0.930	0.441	0.524	0.267	0.625	K23489	0.933	0.547	0.760	0.064	0.228
V28-35	0.956	0.955	0.141	0.032	0.152	K23518	0.927	0.013	0.374	0.872	0.161
V28-36	0.981	0.953	0.252	0.016	0.093	K23519	0.974	−0.001	0.387	0.899	0.130
V28-38	0.946	0.615	0.472	0.070	0.584	K23522	0.985	−0.018	0.473	0.865	0.115
V28-39	0.961	0.657	0.349	−0.014	0.638	K23523	0.984	−0.038	0.413	0.893	0.119
V28-41	0.975	0.628	0.488	0.190	0.553	K23524	0.978	−0.025	0.495	0.848	0.109
V28-42	0.899	0.514	0.462	0.070	0.645	K23525	0.967	−0.019	0.372	0.905	0.098
V28-44	0.950	0.619	0.418	−0.019	0.626	K23526	0.970	0.010	0.420	0.879	0.146
V28-46	0.957	0.453	0.557	0.270	0.607	K23528	0.977	0.002	0.483	0.856	0.112
V28-51	0.974	0.745	0.489	0.147	0.398	K23536	0.856	0.110	0.351	0.767	0.366
V28-52	0.915	0.541	0.463	0.196	0.607	K23549	0.963	0.380	0.863	0.070	0.263
V28-53	0.980	0.469	0.543	0.368	0.574	PS2613	0.962	0.324	0.889	0.089	0.243
V28-55	0.975	0.701	0.309	0.048	0.621	PS2616	0.959	0.363	0.863	0.099	0.269

Table 4. Continued.

Station	Communality	Factor 1	Factor 2	Factor 3	Factor 4	Station	Communality	Factor 1	Factor 2	Factor 3	Factor 4
V28-56	0.956	0.689	0.467	0.118	0.500	PS2644	0.918	0.536	0.701	0.253	0.273
V28-58	0.967	0.917	0.148	0.169	0.274	PS2645	0.970	0.537	0.776	0.228	0.165
V28-59	0.967	0.823	0.335	0.080	0.414	V27-60	0.954	0.617	0.366	0.140	0.648
V28-60	0.974	0.751	0.336	0.166	0.519	V27-63	0.967	0.520	0.448	0.169	0.684
V28-60A	0.954	0.752	0.220	0.190	0.552	V27-69	0.950	0.732	0.413	0.095	0.484
V29-208	0.944	0.859	0.155	0.118	0.409	V27-74	0.945	0.617	0.542	0.327	0.404
V29-209	0.913	0.748	0.258	0.058	0.533	V27-75	0.941	0.733	0.466	0.196	0.385
V29-210	0.945	0.802	0.289	0.198	0.423	V27-76	0.948	0.702	0.416	0.226	0.481
V29-211	0.975	0.807	0.372	0.036	0.429	V27-80	0.934	0.681	0.479	0.238	0.430
V29-219	0.964	0.671	0.392	0.119	0.588	V27-96	0.939	0.541	0.271	0.269	0.707
V29-220	0.965	0.682	0.262	0.161	0.637	V28-17	0.953	0.828	0.445	0.052	0.259
V30-125	0.879	0.127	0.470	0.686	0.414	V28-21	0.984	0.823	0.477	0.102	0.262
V30-130	0.959	0.923	0.229	−0.028	0.234	V28-26	0.944	0.866	0.355	0.005	0.259
V30-131	0.984	0.970	0.144	0.083	0.123	V28-48	0.965	0.587	0.493	0.226	0.572
V30-132	0.973	0.833	0.284	0.285	0.344	V28-49	0.934	0.641	0.548	0.255	0.397
V30-133	0.948	0.729	0.332	0.126	0.540	V30-163	0.898	0.387	0.524	0.188	0.662
V30-135	0.978	0.932	0.284	0.048	0.160	V30-142	0.971	0.626	0.651	0.162	0.360
V30-167	0.959	0.481	0.442	0.146	0.715	V30-143	0.920	0.728	0.375	0.269	0.421
V30-169	0.928	0.443	0.556	0.216	0.613	V30-144	0.955	0.709	0.475	0.275	0.388
V30-170	0.961	0.412	0.432	0.335	0.702						
V30-175	0.959	0.453	0.464	0.198	0.706	Variance		39.331	31.412	9.272	15.395
HM31-35	0.943	0.656	0.401	0.107	0.584	Cum. variance		39.331	70.743	80.015	95.409
K31/2	0.963	0.102	0.754	0.585	0.208						

Spearman rank-order coefficient and the unweighted pairs clustering method is that they are not too much affected by large variations in species abundances and by the distribution of rarer taxa, and are therefore commonly used in palaeo-ecology (Sneath & Sokal 1973).

All data presented in this paper are available in electronic format from the Pangaea databank at http://www.pangaea.de

RESULTS

FACTOR ANALYSIS

The first four factors (assemblages) explain 95.41% of the total information contained in the data set (Table 3), and we interpret them as representing distinct oceanographic, sedimentological and/or opal preservation provinces. The temperature regression equation has a standard error of estimate of $\pm1.2°C$ (Table 3, Fig. 3) and a multiple correlation coefficient of 0.88. Most of the residuals (actual minus estimated temperature value for all core-tops) are <2°C.

The resulting varimax factor components (Table 4) are plotted by stations in a set of maps (Figs 4–7) to facilitate the geographical interpretation of the extracted factors.

We interpreted factor 1 (Fig. 4) as a cold (Polar and Arctic) water factor, because high (>0.80) factor loadings are found on the Iceland Plateau. In the southern portion of the study area (south of *ca* 70°N) factor loadings >0.40 are located on the Iceland Plateau and on the northern side of the Iceland–Faeroe Ridge until about 2°E. Similar high values are also found in the eastern part of the Greenland Sea in a southeast–northwest trending zone. Values higher than 0.50–0.60 approximately trace the position of the Arctic Front and the intrusion of the cold East Iceland Current towards the southern sector of the Norwegian Basin. *Amphimelissa setosa* dominated this factor with a varimax factor score of 4.732 (Table 3). Other important species in factor 1 are the *Pseudodictyophimus gracilipes* group (2.034) and *Lithocampe platycephala* (1.731).

Factor 2 (Fig. 5) was best described as a Greenland Sea factor, as loadings higher than 0.80 are to be found along a southwest–northeast trending belt going from Scoresby Sound on the eastern coast of Greenland to the western coast of Spitsbergen. We associate this pattern with the gyre where branches of cold and warm currents mix to the north of Mohns Ridge and to the west of Knipovich Ridge. Similar high values are also present in the northern part of the Lofoten Basin, approximately located over the Mohns Ridge. High absolute values (Table 3) of varimax scores (4.588) were obtained for the *Actinomma leptoderma/boreale* group, *Actinomma leptoderma longispina* (1.861) and *Larcospira minor* (1.798). Bjørklund & al. (1998) observed that the relative abundances of *Actinomma leptoderma* increased towards the ice-edge off Greenland. This

observation is also in accordance with those of Swanberg & Eide (1992), who found *Actinomma leptoderma* to be one of the dominant species of living plankton in this area.

Factor 3 (Fig. 6) is particularly well represented in the North Atlantic, southwest of Iceland, where factor component values >0.80 are to be found, while values >0.30 are consistently present in the eastern part of the
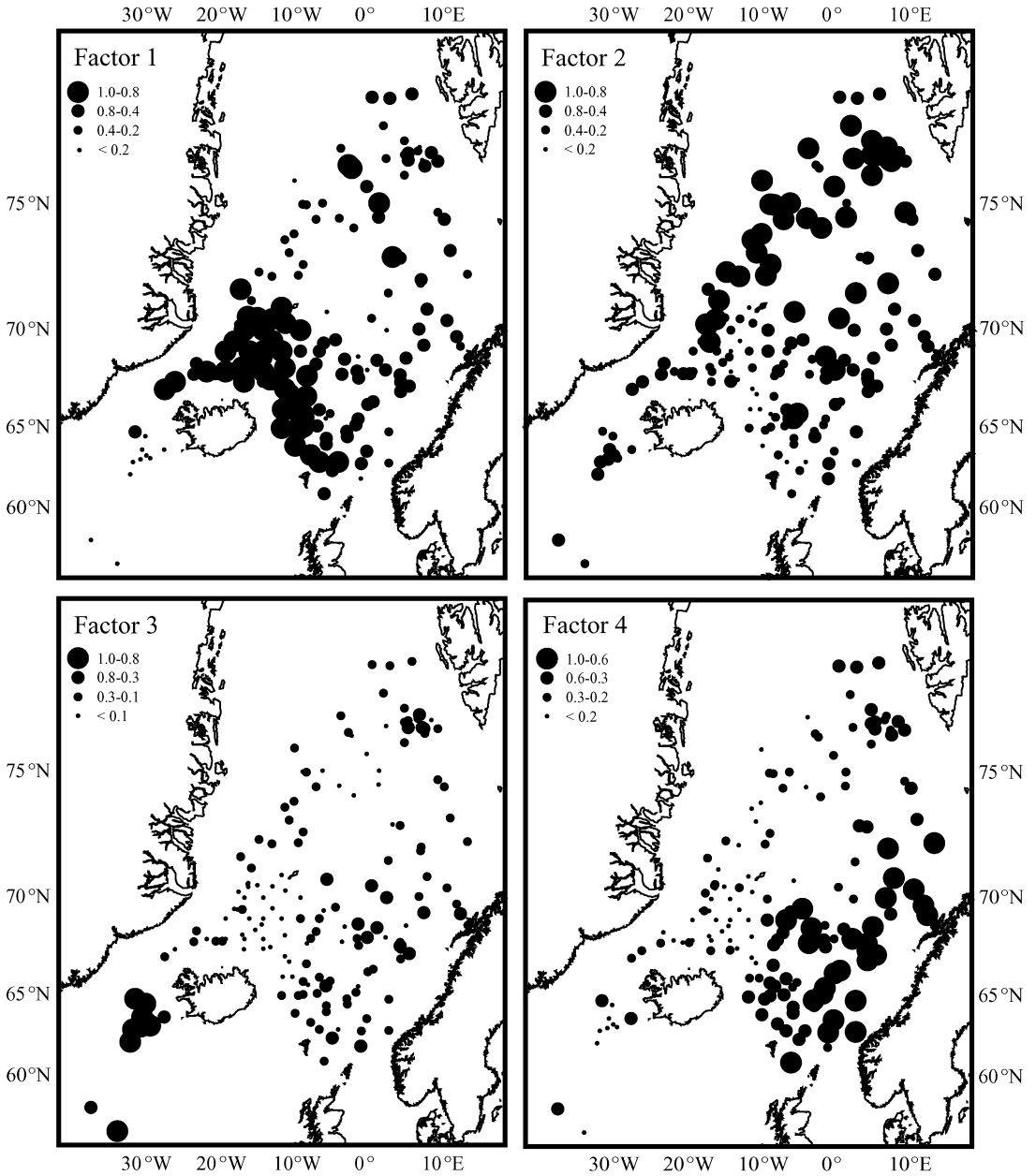
Fig. 4. Varimax factor components for factor 1.
Fig. 5. Varimax factor components for factor 2.
Fig. 6. Varimax factor components for factor 3.
Fig. 7. Varimax factor components for factor 4.

GIN Seas (Norway and Lofoten Basins and off Spitsbergen). These areas are under the influence of warm waters, as the Irminger current flows in the waters southwest of Iceland, and the Norwegian Current (the northward-bound branch of the Gulf Stream) flows offshore Norway in the eastern GIN Seas. *Larcospira*

minor (3.421), the *Spongotrochus* group (*Spongotrochus glacialis + Spongopyle osculosa + Spongodiscus resurgens*) (3.294), and *Phorticium pylonium* (*clevei*) (1.956) were the species with the highest scaled varimax factor scores (Table 3).

Factor 4 (Fig. 7) has been interpreted as a warm
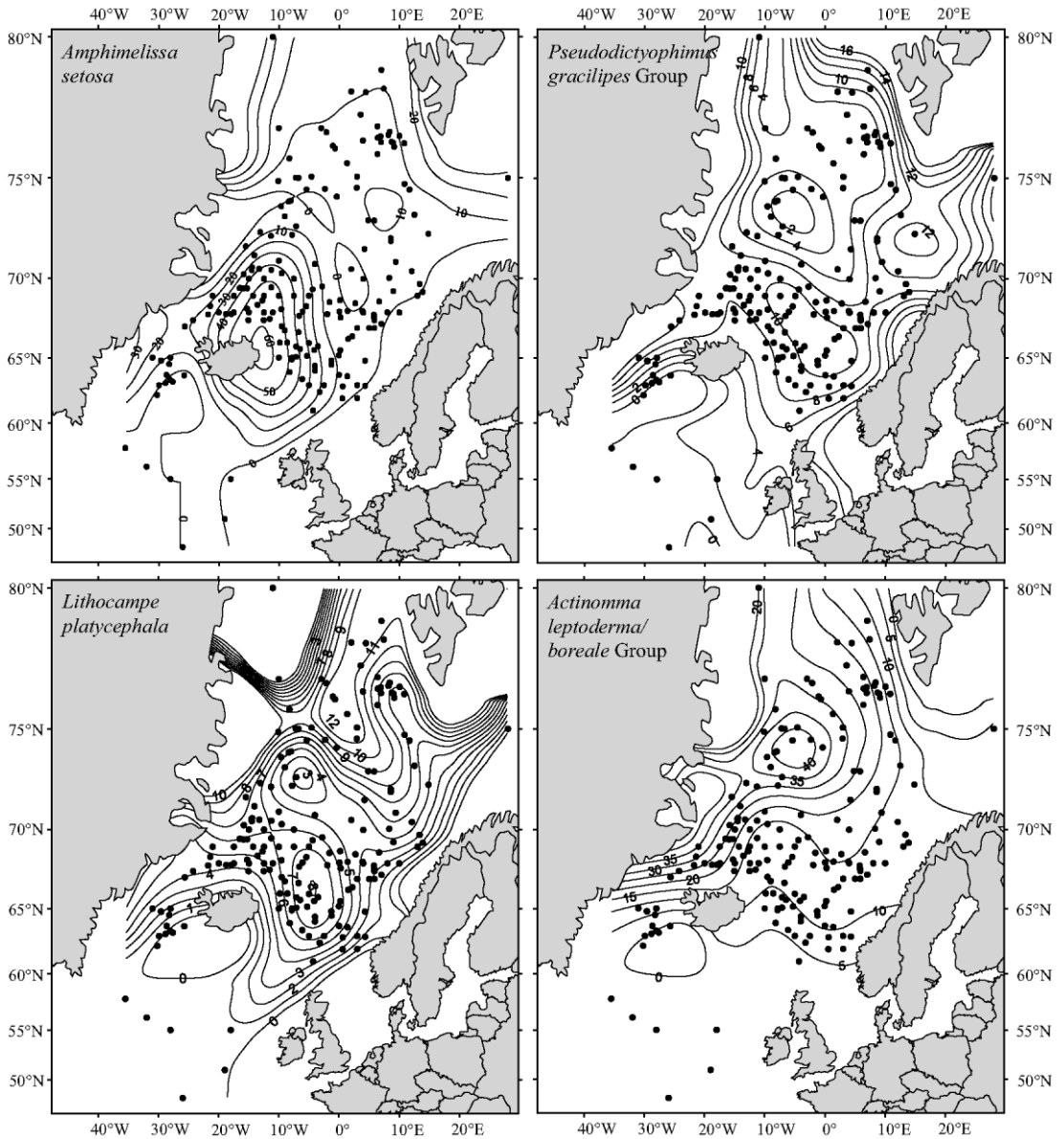
Fig. 8. Relative abundance of *Amphimelissa setosa* in surface sediments.
Fig. 9. Relative abundance of the *Pseudodictyophimus gracilipes* group in surface sediments.
Fig. 10. Relative abundance of *Lithocampe platycephala* in surface sediments.
Fig. 11. Relative abundance of the *Actinomma leptoderma/boreale* group in surface sediments.

(Atlantic) water factor, with particularly high (>0.60) factor loadings off the west coast of Norway, underlying the warm Norwegian Current, which sends off a gyre to the northwest, reaching just to the southeast of Jan Mayen (Fig. 2). This gyre is visible in the lobate shape (overlying the Norway Basin) of the factor loadings distribution for factor 4 (Fig. 7). Species with a high varimax factor score (Table 3) included *Lithomelissa setosa* (3.683), *Artobotrys boreale* (2.388) and the *Pseudodictyophimus gracilipes* group (1.577). The relative abundances of the species having high factor loadings in
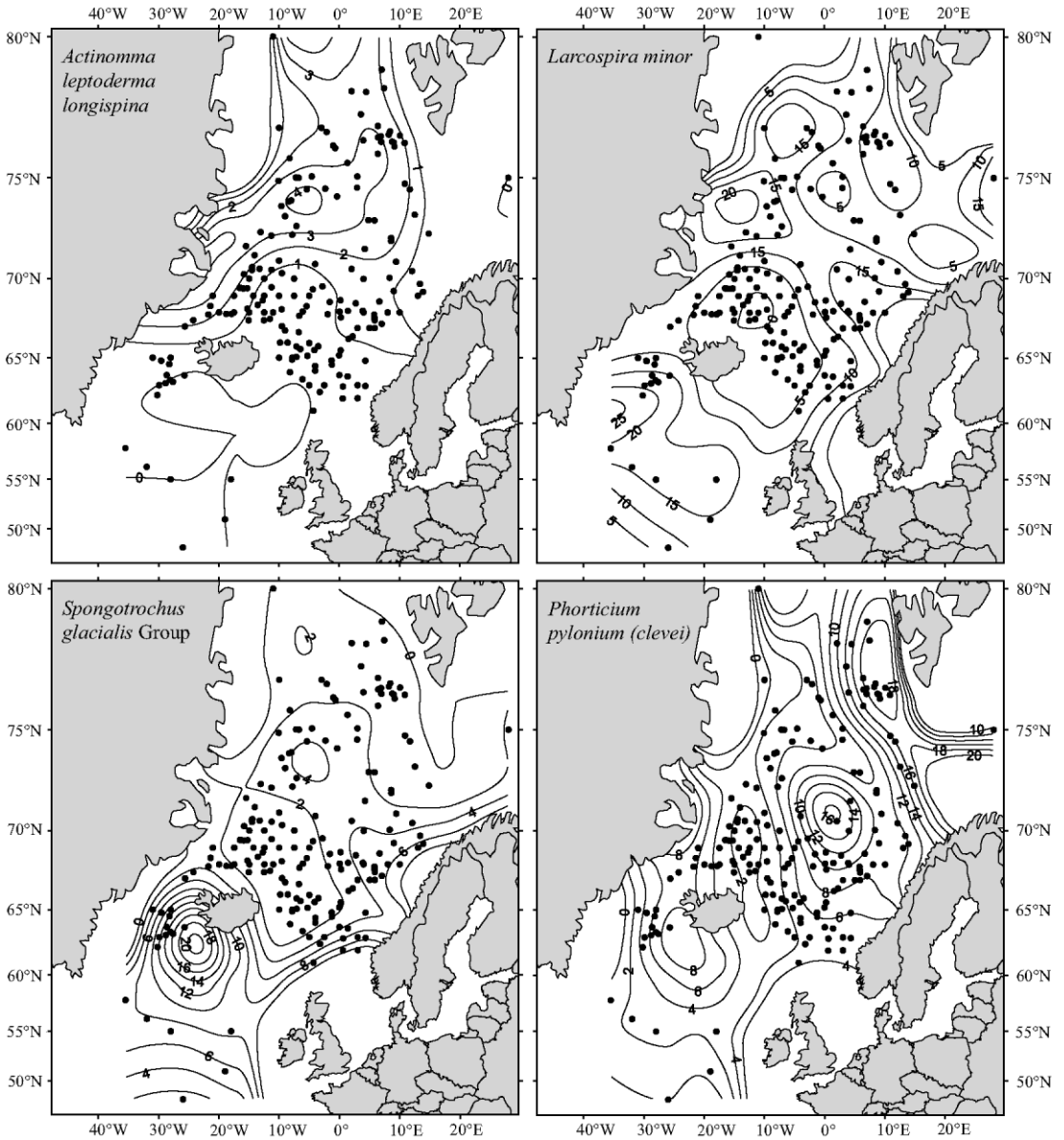
Fig. 12. Relative abundance of *Actinomma leptoderma longispina* in surface sediments.
Fig. 13. Relative abundance of *Larcospira minor* in surface sediments.
Fig. 14. Relative abundance of the *Spongotrochus glacialis* group in surface sediments.
Fig. 15. Relative abundance of *Phorticium pylonium* (*clevei*) in surface sediments.
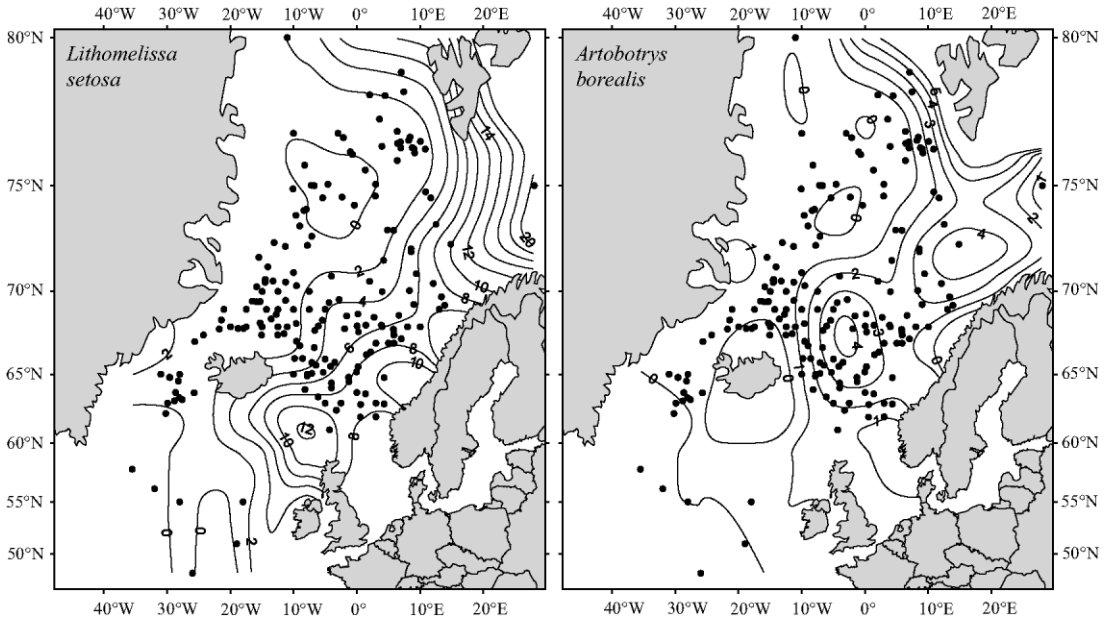
Fig. 16. Relative abundance of *Lithomelissa setosa* in surface sediments.
Fig. 17. Relative abundance of *Artobotrys borealis* in surface sediments.

the four core-top assemblages recognized by factor analysis are shown in Figs 8–17.

CLUSTER ANALYSIS

Cluster analysis was used to supplement the results obtained by Q-mode factor analysis, in order to test the robustness of the groupings obtained by the latter technique. There is very close agreement between the two techniques, as the four station clusters (Fig. 18) are easily comparable with the faunal assemblages recognized by factor analysis (Figs 4–7).

In particular, cluster A stations are mostly located over the Iceland Plateau and their geographical distribution matches the one of factor 1 (Fig. 4), including the presence of this cluster in a few stations to the southwest of Spitsbergen.

Cluster B is the counterpart of factor 4 (Fig. 7), and is centred in the eastern sectors of the Norway and Lofoten Basins, off the west coast of Norway.

Cluster C is very similar to factor 2 (Fig. 5), as its stations are distributed over the Greenland Sea and the western portions of the Norway and Lofoten Basins.

Cluster D resembles factor 3 (Fig. 6), as they are both located in the area to the southwest of Iceland.

The application of the same clustering method and
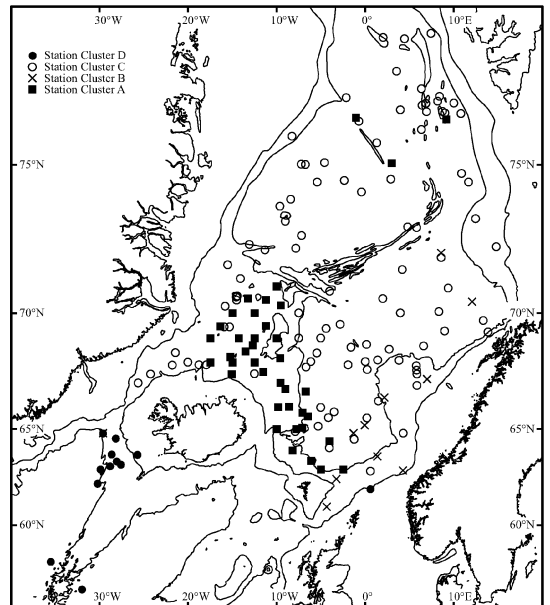
Fig. 18. Geographical distribution of the four clusters of core-top stations recognized by applying cluster analysis (unweighted pair grouping method and Spearman rank-order correlation coefficient) to the reference data set also used for Q-mode factor analysis. The 500 and 2000 m isobaths are also shown.

similarity index to the transposed data matrix (Fig. 19) yields results which are comparable with what we would have obtained by R-mode factor analysis (i.e. which species are important in which station cluster/ area).

We have labelled the four main clusters according to their geographical interpretation (Fig. 19), resulting in (from top to bottom):

- A Greenland Sea species cluster, including *Larcospira minor, Phorticium pylonium* (*clevei*), *Streblacantha circumtexta, Actinomma leptoderma longispina* and the *Actinomma leptoderma/boreale* group, corresponding to station cluster C;
- An Iceland Plateau species cluster, including *Amphimelissa setosa* and *Sethoconus tabulatus*, corresponding to station cluster A;
- A Norwegian Sea species cluster, including *Actinomma* sp. 1, *Plagiacantha arachnoides, Artobotrys borealis, Lithomitra lineata, Artostrobus joergenseni*, the *Pseudodictyophimus gracilipes* group, *Tholospyris gephyristes, Lithocampe platycephala, Plectacantha oikiskos, Ceratocyrtis galeus, Ceratocyrtis histricosus, Lipmanella xiphephorum, Corocalyptra craspedota, Lithomelissa setosa, Lithomelissa hystrix, Lithomelissa thoracites, Lithomelissa* sp. aff. *L. stigi*, corresponding to station cluster B;
- A North Atlantic species cluster, including *Actinomma medianum, Actinomma* sp. 2, the *Spongotrochus glacialis* group, *Eucyrtidium calvertense, Phorticium* sp. 1, *Stylatractus* sp. 1, the drift fauna (*Spongocore puella, Theocorythium trachelium, Lamprocyclas maritalis* and *Euchitonia* spp.), Larcoidea sp. 1, *Lithelius spiralis, Streblacantha* sp. 1, corresponding to station cluster D.

NUMBER OF POLYCYSTINE RADIOLARIANS PER GRAM BULK SEDIMENT

The geographical distribution of the number of polycystine radiolarians per gram bulk sediment (Fig. 20) can give indications on a variety of processes, such as the production of radiolarians in the water column, export efficiency of their skeletons to the sediment, chemical dissolution/terrigenous dilution mechanisms at the seafloor. In order to separate between these processes, additional information is necessary (see Discussion).

In the study area, abundant (generally more than 10,000) radiolarian skeletons per gram bulk sediment are found in the North Atlantic, to the southwest of Iceland, on the Iceland Plateau, and in the Norwegian Sea. Intermediate values (generally less than 1000) are found in the Lofoten Basin, with higher values along the flow pattern of the Norwegian Current (Fig. 2). Low values (barren to less than 1000) are reported from the Greenland Basin, the Barents Sea, as well as from the slope off Scoresby Sound (Greenland).

PHAEODARIA RELATIVE ABUNDANCE

The pattern of Phaeodaria relative abundance (Fig. 21) can provide insights into existing preservation/dissolution provinces (see Discussion), as their skeleton is more unstable (containing less opaline silica) and therefore more easily dissolved than polycystine radiolarians.

The geographical distribution of Phaeodaria in the sediment (Fig. 21) of the GIN Seas is approximately equivalent to the one for the number of radiolarians per gram bulk sediment (Fig. 20). In fact, abundances higher than 1% are almost exclusively found on the Iceland Plateau, in the Norwegian Sea, and in the Lofoten Basin (limited to the area influenced by the Norwegian Current). Moreover, Phaeodaria are virtually absent in the sediments from the Greenland Sea, the Barents Sea, and off Scoresby Sound. The two abundance patterns diverge significantly in both the North Atlantic southwest of Iceland, and on the Vøring Plateau, where the absence of Phaeodaria in the sediment is not matched by the relatively abundant number of radiolarians per gram bulk sediment.

DISCUSSION

TEMPERATURE

The Norwegian Sea is mostly influenced by warm water from the North Atlantic, while the Greenland Sea and the Iceland Plateau are under the influence of cold Polar and Arctic waters. It is therefore to be expected, as stated by Briggs (1995), that temperature is the most important ecological factor in determining the global distribution, or biogeography, of plankton (in this case radiolarian species) in the surface waters, which is also traceable in the distribution pattern of radiolarian skeletons in the bottom sediments.

As an example, in the GIN Seas, we find *Lithomelissa setosa* and *Larcospira* sp. 1 to be more abundant in sediments underlying warm water (Norway Basin), while the *Actinomma leptoderma/boreale* group and *Amphimelissa setosa* are most abundantly found in sediments underlying cold waters (in the Greenland Sea and the Iceland Plateau, respectively). Other taxa, like *Artobotrys borealis, Lithomitra lineata* and the *P. gracilipes* group, are interpreted as Arctic (and there-
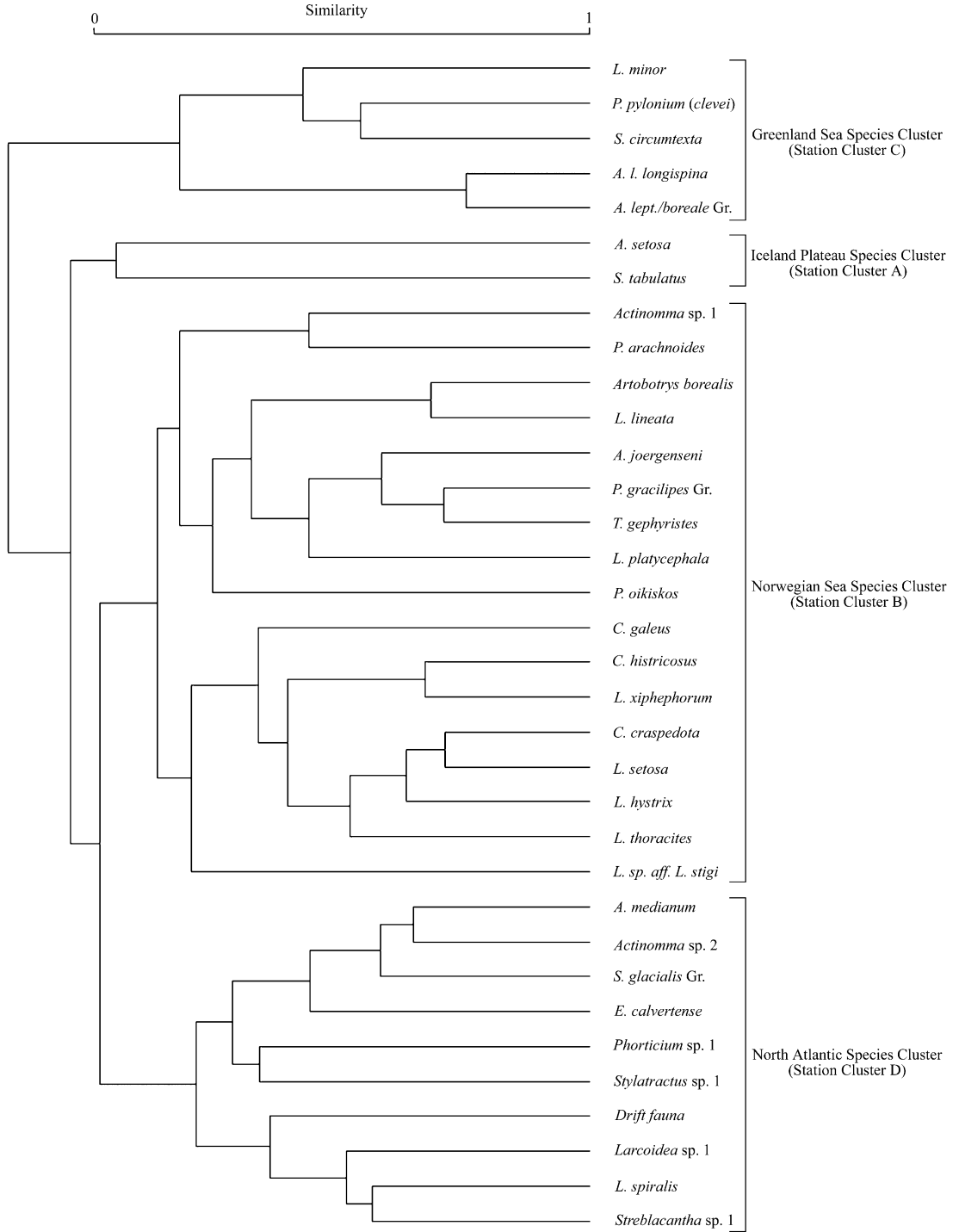
Fig. 19. Cluster analysis for the transposed matrix of the reference data set (species clusters). The square brackets mark the inferred geographical area of importance for the species included in the main four clusters. Also reported (in parentheses) the roughly corresponding station clusters.
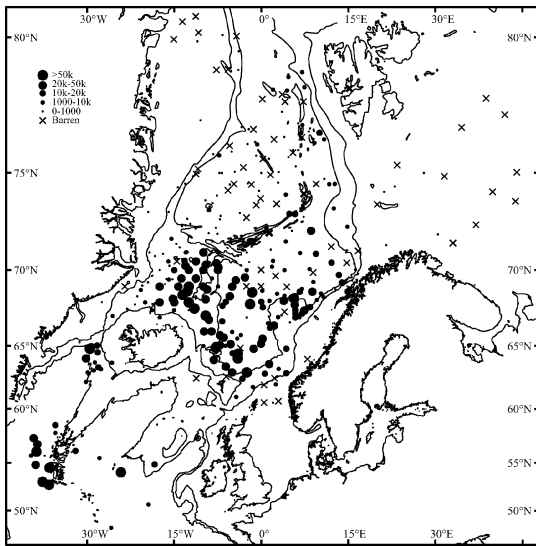
Fig. 20. Abundance of polycystine radiolarians in the surface sediments of the Nordic Seas, expressed as the number of individuals per gram bulk sediment. The 500 and 2000 m isobaths are also shown.

fore adapted to relatively cold surface waters), but with a wide distribution (Schröder-Ritzrau & al. 2001).

PRODUCTION AND PRESERVATION

The degree of preservation of the fossil assemblages is also important in the recognition of biogeographical patterns in bottom sediment studies, and in certain areas it might distort the primary association between plankton species and surface hydrography.

The faunal assemblage in bottom sediments represents an altered version of the plankton assemblage produced in the overlying surface waters. The faunal signature of a locality is generated by microplankton production at the surface, dissolution of the skeletons through the water column and at the water–sediment interface, as well as redeposition and sedimentary processes occurring at the bottom.

Machado da Costa (1993) estimated a 50–86% loss in opal export from the photic zone to the 500 m sediment trap in the Norwegian Sea due to dissolution, and less than 1% of the opal production is incorporated in the sediments. This discrepancy between faunal/floral assemblages in the plankton and in the sediments is, to a different extent, a feature of all plankton groups.

Polycystine radiolarian species have different preservation potential: *Amphimelissa setosa* is an example of a delicate form, while the *Actinomma leptoderma/*

boreale group and *Phorticium pylonium* (*clevei*) are much more robust forms. The distribution of *Amphimelissa setosa* in the bottom sediments of the GIN Seas (Fig. 8) is centred on the Iceland Plateau, an area characterized by good opal preservation, while the *Actinomma leptoderma/boreale* group (Fig. 11) and *Phorticium pylonium* (*clevei*) (Fig. 15) are more abundant in sediments from the Greenland Sea and Lofoten Basin, which are characterized by poor opal preservation.

High production areas such as the Bering Sea export as much as 17.6–44.5 g m^{-2} a^{-1} biogenic opal (Takahashi 1997). In comparison, the GIN Seas have a subdued production regime: the annual export of biogenic opal is relatively low in the Norwegian Sea, 0.5–1.22 g m^{-2} a^{-1} (van Bodungen & al. 1995), while it is 0.7–2.3 g m^{-2} a^{-1} for the Greenland Sea (Ramseier & al. 1999). These are small values compared with the Bering Sea, but the difference between the Norwegian Sea and the Greenland Sea fluxes is significant.

The portion of this flux pertaining to radiolarians is
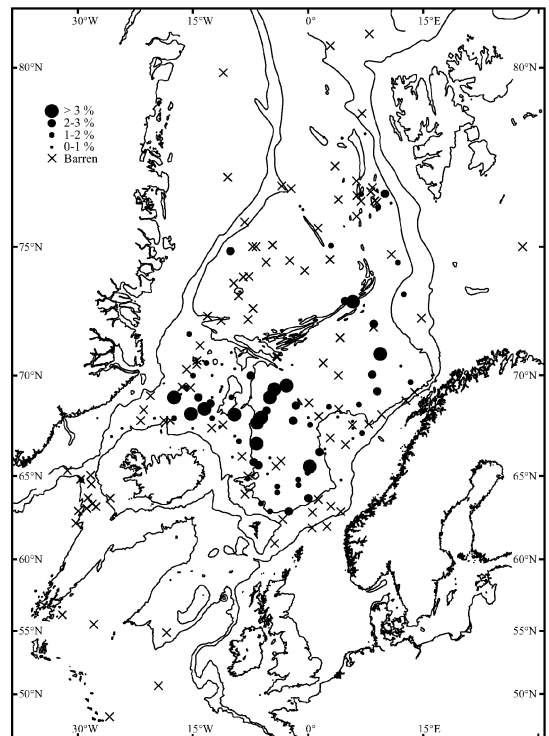
Fig. 21. Abundance of phaeodarian radiolarians in the surface sediments of the Nordic Seas, expressed as the percentage of total radiolarian counts. The 500 and 2000 m isobaths are also shown.

estimated via sediment trap studies. Schröder-Ritzrau & al. (2001) observed that the radiolarian flux in the Greenland Sea was *ca* 2.7×10^{-3} individuals m^{-2} day^{-1}, while in the Norwegian Sea the flux was reduced to *ca* 1×10^{-3} individuals m^{-2} day^{-1}.

The higher opal (and radiolarian) fluxes in the Polar and Arctic waters, than in the Norwegian Sea, are not reflected in the surface sediments (Schröder-Ritzrau & al. 2001). Matthiessen & al. (2001) therefore concluded that preservation limits the applicability of siliceous sediment assemblages in regions which are influenced by cold surface waters, in this case the Greenland Sea.

However, Kohly (1998) observed that even if the main flux species of diatoms and radiolarians are not preserved in the sediments, the heavily silicified post-bloom diatom species are dominant members of deep sediment traps and sediment assemblages.

Radiolarian sediment trap data support the occurrence of strong dissolution in the Greenland Sea: Schröder-Ritzrau & al. (2001) report that the assemblage of polycystine radiolarians in the water column is dominated, in the Greenland Sea, by *Amphimelissa setosa*, with up to 88% of the cumulative flux (37–56% in the Jan Mayen Current). In the sediments, according to our data, the abundance of this species drops to well below 30% in most of the Greenland Sea, and never exceeds 76% in the bottom sediment samples at any location in the GIN Seas. Therefore, our data are in accordance with the observation that *Amphimelissa setosa*, the most dominant species in the plankton, does not survive the settling time through the water or the exposure time at the sediment/water interface, and is mostly dissolved before being incorporated in the sediment (Schröder-Ritzrau & al. 2001).

Our data also indicate that the actinommids (the *Actinomma leptoderma/boreale* group) and larcoids (*Phorticium pylonium* (*clevei*), *Larcospira minor*) are also strongly enriched in the Greenland Sea sediments (14.4 and 40.9%, respectively), compared with the plankton assemblages, where they are both present with 1.3% [average of sediment trap OG 3 and OG 5 data from Schröder-Ritzrau (1995)].

In the specific case of radiolarians from the GIN Seas, we believe that the small portion of produced biogenic opal that is incorporated in the sediment still keeps primary information about the surface waters where radiolarians used to live before settling through the water column and being incorporated in the sediment. This is also indirectly demonstrated by the fact that our temperature regression equation (Table 3) has a high multiple correlation coefficient (0.88) and a low standard error of estimate ($\pm 1.2°$C).

In contrast to the "poor opal preservation" Greenland Sea, the Norwegian and Iceland Seas are exceptional in preserving phaeodarian skeletons (Stadum & Ling 1969; Bjørklund 1984). These skeletons are constructed of amorphous silica with traces of magnesium, calcium and copper (Reschetnyak 1966), and with an organic compound or matrix that is poorly understood (Kling & Boltovskoy 1999). Finally, the spines are hollow and some species have a bubbly, very sensitive to dissolution, "styrofoam" structured skeleton. In Fig. 21 we have plotted the percentage values of phaeodarian skeletons in the sediment. They are essentially not preserved on the western side of the mid-oceanic ridge system, confirming that dissolution is quite active in the Greenland Sea (Schröder-Ritzrau & al. 2001).

Another main difference between the western and eastern GIN Seas consists in the fact that the Greenland Sea includes a sea–ice zone and a marginal ice zone, both characterized by highly stratified water masses and a strong haline stratification, while the adjacent open sea is not influenced by melt water and therefore not stratified.

The number of polycystine radiolarian specimens per gram bulk sediment (Fig. 20) can be used to define oceanic/sedimentary provinces in the GIN Seas, provided that this information is integrated with a general knowledge of processes such as sediment transport and sources, productivity regimes, and surface currents in this region.

In fact, areas with low radiolarian numbers in bottom sediments are usually associated with clear signs of dissolution of opal microfossils (Goll & Bjørklund 1971). Poor preservation of radiolarian skeletons in the GIN Seas is a widespread phenomenon: Bjørklund (unpublished data) observed poorly preserved specimens even from high abundance areas on the Iceland Plateau. Specimens of *Lithocampe platycephala* and *Amphimelissa setosa* had dissolution pits on the surface of the skeleton. These pits extended inwards, giving an almost hollow or tube-like appearance to the skeleton. This seems to take place all over the investigated area, but more so in the radiolarian low abundance areas. We notice, for example, that there is an enrichment of species with heavily silicified skeletons, interpreted by us to be dissolution resistant species (the *Actinomma leptoderma/boreale* group, *Phorticium pylonium* (*clevei*), *Larcospira minor*, the *Spongotrochus glacialis* group) in station clusters C and D, Greenland Sea/ northwestern Lofoten Basin and North Atlantic, respectively (Fig. 18), and by the disappearance, in the bottom sediments of the Greenland Sea, of *Amphimelissa setosa* and *Plectacantha oikiskos*, two species which are reported to be common in the plankton at the ice-edge in the Greenland Sea (Swanberg & Eide 1992).

The distribution of both station clusters (Fig. 18) and radiolarian abundances (Fig. 20) can help to evaluate the influence of preservational processes, bottom topography, and radiolarian production in the study area.

Cluster A occupies the Norway Basin and the Iceland Plateau, bordered by the Iceland–Faeroe Ridge to the south, the Jan Mayen Fracture Zone to the north, the Iceland–Jan Mayen Ridge to the west, and by the 1500 m isobath to the east. Higher than average abundance values in the Iceland Plateau and in the Norway Basin (values >50,000 radiolarians g^{-1} are exclusively found in these areas, Fig. 20) are an effect of high production and effective screening of ice-rafted material from the west. This cluster can be roughly separated, along the 7°W meridian, in a "shallow and cold" Iceland Plateau cluster to the west, and a "deep and warm" Norway Basin cluster to the east.

Cluster B is located along the western coast of Norway, i.e. in the eastern part of the Norway and Lofoten Basins. Radiolarian abundances are higher in the southern part of this cluster and decrease northwards (Fig. 20). This cluster crosses several bathymetric features (Norway and Lofoten Basins, separated by the Jan Mayen Fracture Zone and the Vøring Plateau) and seems to depict the path of the warm Norwegian Current. We therefore assume that primary production is the most important influence on radiolarian abundances in the southern end of cluster B, while terrigenous input and/or bathymetry are most important in the northern end. The high terrigenous input and the frequently observed turbidites in sediment cores in the Lofoten Basin (Kellogg 1976) support this statement.

Cluster C is generally found west of the mid-Atlantic Ridge, in the Lofoten Basin, and in the deepest part of the Norway Basin. The low radiolarian abundances west of the ridge (Greenland and Boreas Basins) are most likely caused by low production (compared with, for example, the Bering Sea), input of terrigenous material from the west by ice-rafting, while in the Lofoten Basin slumping from the continental slope could be the dominating process. Additionally both areas are exposed to active opal dissolution, both in the water column and at the sediment/water interface. In the Greenland Sea, cluster C is aligned on a southwest–northeast trending belt, whose western boundary closely resembles the summer ice-edge position.

The close relationship between cluster C, low radiolarian abundances and high minerogenic input seems to be confirmed by the fact that stations having few radiolarians (barren to less than 1000 radiolarians g^{-1}) are located in shallow areas, such as the North Sea, the Barents Sea and along the east coast of Greenland (Fig. 20). Barren stations are also found at depth in the Lofoten, Greenland and Boreas Basins.

Cluster D is found in the North Atlantic, on the Reykyanes Ridge. Even if the number of radiolarians is high in this area, the opal refractive index is high too, a typical feature of dissolved assemblages (Goll & Bjørklund 1971). This is also in harmony with the low number of Phaeodaria (Fig. 21), another indicator of poor preservation, found in sediment samples from this area.

CONCLUSIONS

- A regression equation for summer sea surface temperature has been developed for the GIN Seas, based on a reference core-top database including 160 stations. The standard error of estimate for this equation is ±1.2°C. This provides an excellent tool for radiolarian-based palaeotemperature estimates in the GIN Seas.
- The distribution of radiolarian species and faunal assemblages in the surface sediments of the Greenland Sea allowed dissolution to be recognized as an important factor in modifying the faunal signal generated in the plankton, without, however, hindering the reliability of the temperature regression equation (multiple correlation coefficient = 0.88 and a standard error of estimate = ±1.2°C).
- Cluster analysis has been applied to the same data set and the results compared with those obtained by factor analysis, the distribution of species relative abundances, prevailing current systems, and preservation provinces in the GIN Seas. This allowed four different factors/assemblages/clusters to be recognized characterizing the different sub-basins in the study area.
- Factor 1 has a very similar distribution to the Iceland Plateau species cluster (station cluster A), and we interpret it as a cold (Polar and Arctic) water factor.
- Factor 2 has a very similar distribution to the Greenland Sea species cluster (station cluster C), and is associated with the gyre formed by the Jan Mayen Current and the Norwegian Current, where cold and warm waters mix.
- Factor 3 has a very similar distribution to the North Atlantic species cluster (station cluster D), associated with the warm Irminger Current southwest of Iceland.
- Factor 4 has a very similar distribution to the Norwegian Sea (Norway and Lofoten Basins) species

cluster, and is associated with the warm water of the Norwegian Current.

REFERENCES

Bailey JW. 1856. Notice of microscopic forms found in the sounding of the Sea of Kamtschatka. *American Journal of Science and Arts* 22(2):1–6.

Bernstein T. 1934. Zooplankton des Nordlischen Teiles des Karisches Meeres. *Transactions of the Arctic Institute* 9:3–58 (in Russian with a German summary).

Bjørklund KR. 1976. Radiolaria from the Norwegian Sea, Leg 38 of the Deep Sea Drilling Project. In: Talwani M & al., editors. *Initial reports of the Deep Sea Drilling Project*. Washington: US Government Printing Office, p. 1101–1168.

Bjørklund KR. 1984. *Euphysetta* (Phaeodaria, Radiolaria) in the Norwegian–Greenland Sea sediments, distribution in space and time. In: Morphology, ecology and evolution. Petrushevskaya MG and Stepanjants SD, editors. *Eurorad IV, Academy of Sciences of the SSSR, Leningrad*, p. 239–244.

Bjørklund KR, Cortese G, Swanberg NR, Schrader HJ. 1998. Radiolarian faunal provinces in surface sediments of the Greenland, Iceland and Norwegian (GIN) Seas. *Marine Micropaleontology* 35:105–140.

Briggs JC. 1995. Global biogeography. *Developments in paleontology and stratigraphy*. Amsterdam: Elsevier, p. 1–452.

Claparède E. 1855. Über die Lebenerscheinungen und insbesonderes Bewegungserscheinungen der Acanthometren. *Bericht über die zur Bekanntmachung geeigneten Verhandlungen der Königliche Preussische Akademie der Wissenschaften zu Berlin*, p. 674–676.

Cleve PT. 1899. Plankton collected by the Swedish expedition to Spitzbergen in 1898. *Küngliga Svenska Vetenskaps Akademiens Handlingar* 32(3):25–51.

Cortese G, Bjørklund KR. 1998. The taxonomy of boreal Atlantic Ocean Actinommida (Radiolaria). *Micropaleontology* 44(2):149–160.

Diepenbroek M, Grobe H, Sieger R. 2000. PanMap. http://www.pangaea.de/Software/PanMap.

Dietrich G. 1969. Atlas of the hydrography of the North Atlantic Ocean. Based on the Polar Front survey of the International Geophysical Year, winter and summer 1958. *ICES Outside Series*, Charlottenlund Slott, Denmark, p. 140.

Dolven JK. 1998. Late Pleistocene to Late Holocene biostratigraphy and paleotemperatures in the SE Norwegian Sea, based on polycystine radiolarians. Master Degree Thesis, Faculty of Mathematics and Natural Sciences, University of Oslo, p. 100.

Dreyer F. 1889. Die Pylombildungen in vergleichend-anatomischer und etwicklungsgeschichtlichen Beziehung bei Radiolarien und bei Protisten ueberhaupt, nebst System und Beschreibung never und der bis jetzt bekannten pylomatischen Spumellarien. *Jenaische Zeitschrift für Naturwissenschaft* 23:77–214.

Ehrenberg CG. 1839. Über die Bildung der Kreidefelsen und des Kreidemergels durch unsichtbare Organismen. *Abhandlungen der Königlichen Akademie der Wissenschaften zu Berlin*, p. 59–147.

Ehrenberg CG. 1854. *Mikrogeologie: Das Erden und Felsen schaffende Wirken des unsichtbar kleinen selbständigen Lebens auf der Erde*. Leipzig (Leopold Voss), p. 374.

Ehrenberg CG. 1862. Die Tiefgrund-Verhältnisse des Ozeans am Eingange der Davisstrasse und bei Island. *Monatsberichte der Königlichen Preussischen Akademie der Wissenschaften zu Berlin*, p. 275–315.

Ehrenberg CG. 1873. Mikrogeologische Studien über das kleinste Leben der Meeres-Tiefgründe aller Zonen und dessen geologischen Einfluss. *Monatsberichte der Königlichen Preussischen Akademie der Wissenschaften zu Berlin*, p. 131–399.

Goll RM, Bjørklund KR. 1971. Radiolaria in surface sediments of the North Atlantic Ocean. *Micropaleontology* 17(4):434–454.

Goll RM, Bjørklund KR. 1974. Radiolaria in surface sediments of the South Atlantic. *Micropaleontology* 20:38–75.

Haeckel E. 1862. *Die Radiolarien (Rhizopoda radiata). Eine Monographie*. Berlin, p. 572.

Haeckel E. 1887. Report on the Radiolaria collected by the H.M.S. Challenger during the years 1873–1876. Report Voyage Challenger. *Zoology* 18:1–1803.

Hammer Ø, Harper DAT, Ryan PD. 2001. Past: Paleontological statistic software package for education and data analysis. *Paleontologica Electronica* 4(1)http://www.erdw.ethz.ch/~pe/toc.htm.

Hülsemann K. 1963. Radiolaria in plankton from the Arctic Drifting Station T-3, including the description of three new species. *Arctic Institute of North America Technical Paper* 13:1–52.

Imbrie J, Kipp NG. 1971. A new micropaleontological method for quantitative paleoclimatology: application to a late Pleistocene Caribbean core. In: Turekian KK, editor. *The late Cenozoic glacial ages*. New Haven, CT: Yale University Press, p. 71–147.

Jørgensen E. 1900. Protistenplankton aus dem Nordmeere in den Jahren 1897–1900. *Bergens Museums Aarbog 1899* 6:45–98.

Jørgensen E. 1905. The protist plankton and the diatoms in bottom samples. In: Nordgaard O, editor. *Hydrographical and biological investigations in Norwegian fiords. Bergens Museum Skrifter*, p. 114–141.

Kellogg TB. 1976. Late Quaternary climatic changes: evidence

from deep-sea cores of Norwegian and Greenland Seas. *Geological Society of America Memoir* 145:77–110.

Kling SA, Boltovskoy D. 1999. Radiolaria Phaeodaria. In: Boltovskoy D, editor. *South Atlantic zooplankton*. Leiden: Backhuys, p. 213–264.

Koç N, Jansen E, Haflidason H. 1993. Paleoceanographic reconstructions of surface ocean conditions in the Greenland, Iceland and Norwegian seas through the last 14 ka based on diatoms. *Quaternary Science Review* 12:115–140.

Koç N, Jansen E, Hald M, Labeyrie L. 1996. Late glacial-Holocene sea surface temperatures and gradients between the North Atlantic and the Norwegian Sea: implications for the Nordic heat pump. *Geological Society Special Publication* 111:177–185.

Koç-Karpuz N, Schrader H. 1990. Surface sediment diatom distribution and Holocene paleotemperature variations in the Greenland, Iceland and Norwegian seas. *Paleoceanography* 5:557–580.

Kohly A. 1998. Diatom flux and species composition in the Greenland Sea and the Norwegian Sea in 1991–1992. *Marine Geology* 145(3–4):293–312.

Machado da Costa E. 1993. Production, sedimentation and dissolution of biogenic silica in the northern North Atlantic. PhD Thesis, University of Kiel, p. 123.

Martin GC. 1904. *Radiolaria*. In: Clark WB, Eastman CR, Glenn LC, Bagg RM, Bassler RS, Boyer CS, Case EC, Hollick CA, editors. *Systematic paleontology of the Miocene deposits of Maryland: Baltimore*. Baltimore: Maryland Geological Survey, Johns Hopkins Press, p. 447–459.

Matthiessen J, Baumann K-H, Schröder-Ritzrau A, Hass C, Andruleit H, Baumann A, Jensen S, Kohly A, Pflaumann U, Samtleben C, Schäfer P, Thiede J. 2001. Distribution of calcareous, siliceous and organic-walled planktic microfossils in surface sediments of the Nordic Seas and their relation to surface-water masses. In: Schäfer P, Ritzrau W, Schlüter M, Thiede J, editors. *The northern North Atlantic: a changing environment*. Berlin: Springer, p. 105–127.

Nigrini C. 1967. Radiolaria in pelagic sediments from the Indian and Atlantic Oceans. *Bulletin of the Scripps Institution of Oceanography* 11:1–125.

Peinert R, Bauerfeind E, Gradinger R, Haupt O, Krumbholz M, Peeken I, Werner I, Zeitzschel B. 2001. Biogenic particle sources and vertical flux patterns in the seasonally ice-covered Greenland Sea. In: Schäfer P, Ritzrau W, Schlüter M, Thiede J, editors. *The northern North Atlantic: a changing environment*. Berlin: Springer, p. 69–79.

Petrushevskaya MG. 1969. Raspredelenie skeletov radioljarij v osadkah severiej Atlantiki. In: Vyalov OS, editor. *Iskopaemye i sovrennye radioljarij*. (Material vtorogo vsesojoenogo seminara po radioljarijam). Vov: University Press, p. 123–132.

Popofsky A. 1908. Die Radiolarien der Antarktis. *Deutsche Zoologische Südpolar Expedition (1901–1903)* 10:185–308.

Ramseier RO, Garrity C, Bauerfeind E, Peinert R. 1999. Sea-ice impact on long-term particle flux in the Greenland Sea's Is Odden-Nordbukta region during 1985–1996. *Journal of Geophysical Research* 104:5329–5343.

Reschetnyak VV. 1966. Deep sea phaeodarian radiolaria of the Northwest Pacific. *Fauna SSSR, New Series* 94:1–208.

Samtleben C, Schäfer P, Andruleit H, Baumann A, Baumann KH, Kohly A, Matthiessen J, Schröder-Ritzrau A. 1995. Plankton in the Norwegian–Greenland Sea: from living communities to sediment assemblages—an actualistic approach. *Geologische Rundschau* 84:108–136.

Schröder-Ritzrau A. 1995. Aktuopaläontologische Untersuchung zu Verbreitung und VerticalfluX von Radiolarien sowie ihre räumliche und zeitliche Entwicklung im Europäischen Nordmeer. *Berichte aus dem Sonderforschungsbereich 313, Kiel University* 52:1–99.

Schröder-Ritzrau A, Andruleit H, Jensen S, Samtleben C, Schäfer P, Matthiessen J, Hass HC, Kohly A, Thiede J. 2001. Distribution, export and alteration of fossilizable plankton in the Nordic Seas. In: Schäfer P, Ritzrau W, Schlüter M, Thiede J, editors. *The northern North Atlantic: a changing environment*. Berlin: Springer, p. 81–104.

Sejrup HP, Haflidason H, Kristensen DK. 1995. Rapid Communication. Last interglacial and Holocene climatic development in the Norwegian Sea region: ocean front movements and ice-core data. *Journal of Quaternary Science* 10(4):385–390.

Sieger R, Gersonde R, Zielinski U. 1999. A new extended software package for quantitative paleoenvironmental reconstructions. *EOS, Transactions, American Geophysical Union*, p. Electronic supplement.

Sneath PHA, Sokal RR. 1973. *Numerical taxonomy: the principles and practice of numerical classification*. San Francisco: Freeman, p. 573.

Stadum CJ, Ling HY. 1969. Tripylean radiolaria in deep-sea sediments of the Norwegian Sea. *Micropaleontology* 15:481–489.

Swanberg NR, Eide LK. 1992. The radiolarian fauna at the ice edge in the Greenland Sea during summer, 1988. *Journal of Marine Research* 50:297–320.

Takahashi K. 1997. Time-series fluxes of Radiolaria in the eastern subarctic Pacific Ocean. *News of Osaka Micropaleontologists*, Special Volume 10:299–309.

van Bodungen B, Anita A, Bauerfeind E, Haupt O, Peeken I, Peinert R, Reitmeier S, Thomsen C, Voss M, Wunsch M, Zeller U, Zeitzschel B. 1995. Pelagic processes and vertical flux of particles: an overview over long-term comparative study in the Norwegian Sea and Greenland Sea. *Geologische Rundschau* 84:11–27.